REPUBLIC OF TURKEY

YILDIZ TECHNICAL UNIVERSITY

GRADUATE SCHOOL OF NATURAL AND APPLIED SCIENCES

AN INVESTIGATION OF SLEEP-ACTIVE NEURONS USING
PHARMACOGENETICS METHODS

ILKE GUNTAN

MSc. THESIS

DEPARTMENT OF BIOENGINEERING

PROGRAM OF BIOENGINEERING

ADVISOR

PROF. DR. DILEK TURGUT-BALIK

CO-ADVISOR

PROF. DR. WILLIAM WISDEN

ISTANBUL, 2014

REPUBLIC OF TURKEY

YILDIZ TECHNICAL UNIVERSITY

GRADUATE SCHOOL OF NATURAL AND APPLIED SCIENCES

AN INVESTIGATION OF SLEEP-ACTIVE NEURONS USING PHARMACOGENETICS METHODS

A thesis submitted by Ilke GUNTAN in partial fulfillment of the requirements for the degree of **MASTER OF SCIENCE** is approved by the committee on 12/06/2014 in Department of Bioengineering.

Thesis Advisor
Prof. Dr. Dilek TURGUT-BALIK
Yıldız Technical University

Co- Advisor
Prof. Dr. William WISDEN
Imperial College London

Approved By the Examining Committee
Prof. Dr. Dilek TURGUT-BALIK
Yıldız Technical University

Prof. Dr. William WISDEN
Imperial College London

Prof. Dr. Barbaros NALBANTOĞLU
Yıldız Technical University

Doç. Dr. Nehir ÖZDEMİR ÖZGENTÜRK
Yıldız Technical University

Assist. Prof. Dr. Alper YILMAZ
Yıldız Technical University

ii

ACKNOWLEDGEMENTS

TABLE OF CONTENTS

LIST OF SYMBOLS

bp   Basepair
g   Gram
kDa   Kilodalton
L   Litre
µg   Microgram
µL   Microlitre
mM   Millimolar
mL   Millilitre
M   Molar
^{o}C   Centigrade degree
V   Volt
Hz   Hertz
µV   Microvolt
$µV^2$ Microvolt squared
γ   Gamma
Δ   Delta
®   Resigtered sign
α   Alpha
x g   Relative centrifugal force
mL/min   Millilitre per minutes
mg/mL   Milligram per millilitre
mg/kg   Milligram per kilogram
kb   Kilobase
U/mL   Units per millilitre
cm^2 Centimeter squared
L/min   Litre per minute
p   *p*-value

LIST OF ABBREVIATIONS

AAV	Adeno-associated virus
Ach	Acetylcholine
AL	Allatostatin
AlstR	Drosophila allatostatin receptor
ARAS	Ascending reticular activation system
BF	Basal forebrain
BG	Basal ganglia
Cing	Cingulate cortex
CNO	Clozapine-*N*-oxide
CNS	Central nervous system
DAPI	4',6-diamidino-2-phenylindole
ddH$_2$O	Double-distilled water
DMEM	Dulbecco's modified Eagle medium
dNTP	Deoxyribonucleotide triphosphate
Dox	Doxycycline
DREADD	Designer Receptors Exclusively Activated by Designer Drug
ECoG	Electrocorticography or intracranial EEG
EEG	Electroencephalography
EMG	Electromyography
EOG	Electrooculography
GABA	γ-aminobutyric acid
GHT	Geniculohypothalamic tract
GPCR	G protein-coupled receptors
HeBS	HEPES buffered saline
Hek293	Human embryonic kidney 293 cells
hM3Dq	human muscarinic subtype 3 G$_q$-coupled DREADD
hM4Di	human muscarinic subtype 4 G$_i$-coupled DREADD
hSyn	Human Synapsin promoter
IEG	Immediate early gene
IgG (H + L)	Immunoglobulin G (heavy and light chain)
IGL	Intergeniculate leaflet
IHC	Immunohistochemistry
ILC	Intermediolateral column of the thoracic chord grey

IP	Intraperitoneal
LC	Locus coeruleus
LGN	Lateral geniculate
LH	Lateral hypothalamus
LHA	Lateral hypothalamic area
M3	Muscarinic subtype 3
MCH	Melatonin concentrating hormone
MEMA	Middle ear muscle activition
ML	Mediolateral
MnPN	Median pre-optic nucleus
MUA	Multi-unit activity
NaCl	Sodium chloride
NGS	Normal goat serum
NREM	Non-rapid eye movement
O_2	Oxygen
ORX	Orexin
PBS	Phosphate buffered saline
PCR	Polymerase chain reaction
PFA	Paraformaldehyde
PGO	Ponto-geniculo-occipital
PINEAL	Pineal gland
POA	Preoptic area
PPT/LDT	Pedunculopontine and laterodorsal tegmental nucleus
PVT	Paraventricular nuclei
RASSLs	Receptors activated solely by synthetic ligands
REM	Rapid eye movement
RHT	Retinohypothalamic tract
RS	Recovery sleep
SCG	Superior cervical ganglion
SCN	Suprachiasmatic nuclei
SD	Sleep deprivation
SDS-PAGE	Sodium dodecyl sulfate polyacrylamide gel electrophoresis
SLD	Sublaterodorsal nucleus
SWS	Slow wave sleep
TMN	Tuberomammillary nucleus
tTA	Tetracycline transactivator
VLPO	Ventrolateral preoptic nucleus
vPAG	Ventral periaqueductal gray matter

LIST OF FIGURES

xii

LIST OF TABLES

ABSTRACT

AN INVESTIGATION OF SLEEP-ACTIVE NEURONS USING PHARMACOGENETIC METHODS

Ilke GUNTAN

Department of Bioengineering

MSc. Thesis

Advisor: Prof. Dr. Dilek TURGUT-BALIK

Co-advisor: Prof. Dr. William WISDEN

There is little known about the neural mechanisms governing how we sleep. In this thesis we were interested in understanding the neurotransmitters and the neural circuitry that are used in the mammalian brain to control sleep and the waking state.

The current major hypothesis, flip-flop model, is that sleep-active GABAergic neurons inhibit arousal neurons throughout the sleep period. To test this hypothesis, sleep-active neurons have been excited or inhibited selectively and reversibly. A binary genetic switch have been constructed; a neuronal activity-inducible gene encoding a transcriptional activator (c-fos promoter linked to TET-activator reading frame) and a gene that encodes the TET protein binding site linked to a reading frame for the G-protein coupled receptors hM3Dq or hM4Di. These two transgene system have been packaged into recombinant adeno-associated viruses (AAV) and delivered into sleep active VLPO region of the brain by stereotaxic injection. It was planned the first transgenic system to drive the second one, *in vivo*. hM3Dq and hM4Di receptors respond to the drug clozapine-N-oxide (CNO), which usually has no targets in the body. CNO administration produced excitation in sleep-active neurons which express the hM3Dq receptor; conversely, hM4Di activation expected to produce inhibition.

Using EEG recordings and animal behavior test, effects of CNO administration has been investigated upon sleep in sleep-deprived mice. It has been understood that selectively

excited sleep-active neurons in VLPO have been able to induce sleep when the animals were wake as flip-flop hypothesis proposed.

Key Words: Sleep-active neurons, VLPO, G-protein coupled receptors, c-fos, CNO

UYKUDA AKTİF OLAN SİNİR HÜCRELERİNİN FARMAKOGENETİK YÖNTEMLERLE İNCELENMESİ

İlke GÜNTAN

Biyomühendislik Anabilim Dalı

Yüksek Lisans Tezi

Tez Danışmanı: Prof. Dr. Dilek TURGUT-BALIK

Eş Danışman: Prof. Dr. William WISDEN

Uykunun sinirsel mekanizması hakkında çok az bilgi mevcuttur. Bu nedenle, bu tezde memeli beyninde uyku ve uyanıklık durumlarını kontrol eden nörotransmiter ve sinirsel devrelerin işleyişlerinin daha iyi anlaşılabilmesi için çalışmalar yürütülmüştür.

Bu konuda şu an için varolan temel hipotez, flip-flop modeli, uykuda aktif olan GABA-erjik sinir hücrelerinin uyku süresince uyarıcı sinir hücrelerini inhibe ettiğini öne sürmektedir. Bu hipotezi test etmek için, uykuda aktif sinir hücreleri seçici ve geri döndürülebilir bir şekilde aktive veya inhibe edilmiştir. Bu amaçla, ikili genetik açma-kapama sistemi oluşturulmuştur; sistemde sinirsel aktivite ile indüklenen ve bir transkripsiyon aktivatörünü kodlayan gen (TET-aktivatör okuma çerçevesine bağlı c-fos promotoru) ve G-proteini reseptörleri olan hM3Dq veya hM4Di'nin okuma çerçevesine bağlanmış TET protein bağlanma bölgesini kodlayan gen bulunmaktadır. Bu iki transgen sistemi rekombinant adeno-ilişkili virüs (AAV) içine paketlenmiştir ve stereotaksik enjeksiyon ile beynin uyku aktif VLPO bölgesine iletilmiştir. İlk transgen sisteminin ikinci transgen sisteminin ekspresyonunu *in vivo* olarak tetiklemesi planlanmıştır. hM3Dq ve hM4Di reseptörleri, normalde vücutta herhangi bir hedefi olmayan klozapin-N-okside (CNO) adlı ilaca yanıt verirler. CNO'nun hM3Dq reseptörlerine bağlanması bu reseptörü taşıyan hücrelerde uyarılmaya neden olurken; hM4Di reseptörünün CNO kökenli aktivasyonu inhibisyonu tetiklemiştir.

EEG ölçümleri ve hayvan davranış testleri yaparak, CNO uygulamasının uyku üzerindeki etkileri uykusuz bırakılmış farelerde incelenmiştir. VLPO'daki uyku-aktif nöronların

seçici bir şekilde uyarılması, flip-flop modelinin önerdiği gibi, farelerde uykuyu tetiklemiştir.

Anahtar Kelimeler: Uyku-aktif sinir hücreleri, VLPO, G-proteini reseptörleri, c-fos, CNO

INTRODUCTION

1.1 Literature Review

1.1.1 Sleep

Sleep described as a reversible loss of wakefulness which is characterized by the change of physiological functions like brain activity, cardiovascular activity, respiration, etc [1]. The characterization of sleep may vary between mammals and non-mammals. However, all species which have shown sleep-like behavior have some similar patterns including unresponsiveness to external stimuli, conservation of a typical posture and choosing a safe site [2].

1.1.1.1 Physiology

Every species show different patterns and amounts of sleep. Sleep characteristics changes continuously and significantly with age in human beings. While infants sleep nearly 16 hours, a normal, healty adult sleep approximately 8 hours over 24 hours. Humans spend one third of their life span by sleeping [2, 3]. Even though, sleeping occupy very important place in our lifes, it is still vague why and how we sleep. With the experiments has been going on more than half a century, scientists found that brain remains highly active when we sleep. Variable brain activity and decreased heart rate, breathing and body temperature are general physiological changes during sleep [2].

There are two phases of sleep, non-rapid eye movement (NREM) sleep and rapid eye movement (REM) sleep (Figure 1.1). Each phase has distinctive features such as variety of brain wave patterns, eye movements and muscle tone [4].
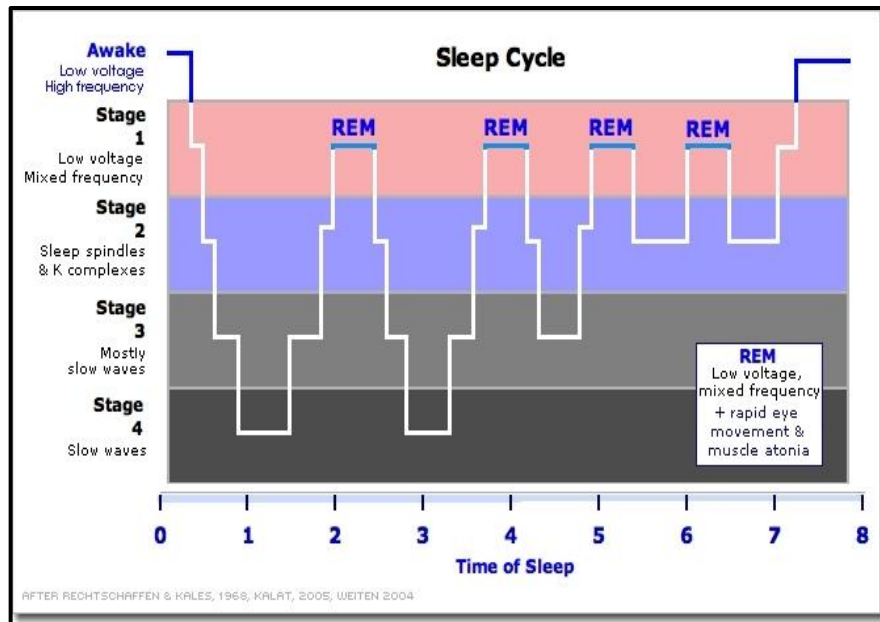
Figure 1. 1 A hpynogram example of a normal, healthy adult [4].

1.1.1.1.1   NREM Sleep

NREM sleep comprises four stages (stages N1, N2, N3 and N4) and each of the stages associate with unique EEG (electroencephalography) patterns. The four NREM stages are roughly relevant with depth of sleep, the arousal threshold increases from stage N1 to stage N4 [1, 4].

During wakefulness, our brain waves comprise of beta and alpha waves. The beta waves are seen when we learn, create, read, write in short while an individual is alerted. The alpha waves is more likely to be seen during resting state or drowsiness. Wake-sleep transition is defined by reduction of alpha waves (Figure 1.2). The subject do not have to be unconscious particularly at sleep onset [5].

Healty adults generally enter sleep with stage N1. N1 sleep is the first step to sleep, typically continues 1 to 7 minutes and comprises 2% to 5% of total sleep. In this stage, it is extremely easy to disrupt one's sleep by a minor stimuli. An increase in percentage of stage N1 indicates disrupted sleep. N1 sleep is identified with low-voltage mixed

frequency EEG activity and a shift from alpha waves (8 to 13 Hz; common in arousal state) to theta waves (4 to 7 Hz) [2].
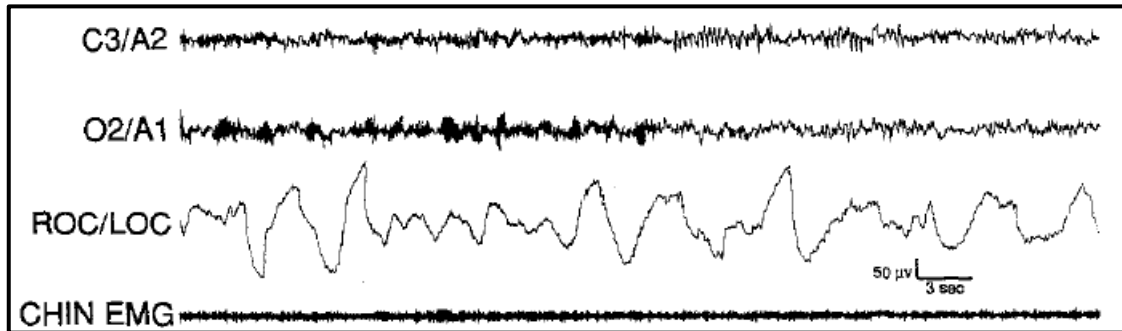
Figure 1. 2 The change in EEG pattern from wakefulness to stage 1 as illustrated here is accepted as sleep onset. The wake stage N1 transition is very clear in EEG channel (C3/A2 and O2/A1) recordings. In the middle of the pattern, brain waves change from alpha waves to theta waves. ROC/LOC: EOG (electrooculography) signals; CHIN EMG: electromyography signals that are taken from chin muscle[1].

Stage N2 of NREM sleep is characterized by sleep spindles (most commonly 12 to 14 Hz) and K-complexes (Figure 1.3). An individual requires moderate stimuli to alter to awake state during N2 sleep. If a minor stimulus is performed, it generally provokes K-complex but not result in wakefulness [1]. N2 is usually continues 10 to 25 minutes and comprises 45-55% of total sleep.

Recently, stage N3 and stage N4 are fused together and started to refer as slow-wave sleep (SWS), delta sleep, or deep sleep. It is very hard to arouse and get back to full wakefulness very quickly during SWS. These two stages are defined by high voltage (≥75 µV) slow wave (≤2 Hz) activity EEG. The distinction between these two stages based on slow wave activity. If slow wave activity covers 20-50% of EEG recording, it is categorized as stage N3. If slow wave activity covers more than 50% of EEG recording, it is categorized as stage N4 [6]. Stage 3 maintains only a few minutes in the first cycle and comprises 3-8% of total sleep while stage 4 typically lasts 20 to 40 minutes and comprises 10-15% of total sleep [1].
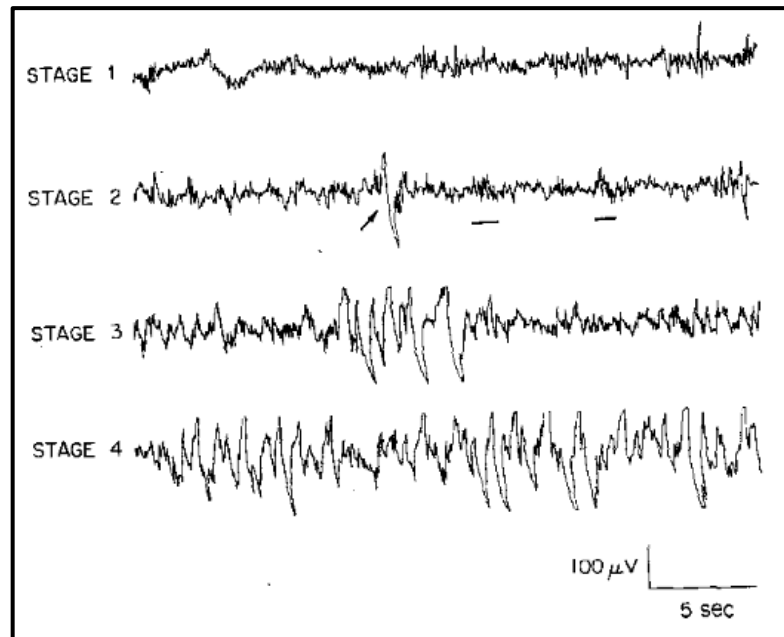
Figure 1. 3 EEG tracings of different stages of NREM sleep. The arrow is pointed K-complex and underlines are indicated sleep spindles [1].

In addition, recently some evidences have been found that there is a connection between sleep spindles and SWS, and declarative memory consolidation [7]. It is known individuals with schizophrenia, alzheimer disease, and fibromyalgia syndrome have a bad quality of NREM sleep. It can be observed significant reduction in sleep spindles and SWS during NREM, as well as poor declarative memory. It is thought to originate from disfunction of thalamus and hypothalamus. As a result, the information can not be project to neocortex for the memory consolidation [8, 9].

Besides neurophysiological changes, other physiological parameters also show particular differentiation. During NREM sleep heart rate slows down and eventually blood pressure and blood flow to brain decreases. The secretion of adrenaline and cortisteroids diminishes and at the same time growth hormone and melatonin secretion is increased in the transition to sleep. The body temperature start to drop as onset of sleep and continue to decrease during sleep. Respiration and metabolic activity also slow down when compared to wake state [2].

1.1.1.1.2 REM Sleep

REM sleep has a very similar EEG pattern with wakefulness and it is really hard to differentiate this pattern only using EEG. Therefore electroencephalography (EEG),

electromyography (EMG) and electrooculography (EOG) generally use together during sleep studies. And also, REM sleep has been alternatively named as paradoxical sleep for this reason [10]. REM sleep is recognized by desynchronized EEG activity, muscle atonia and rapid eye movements. REM sleep comprises %20-25 of total sleep. First REM episode in first cycle of sleep is usually very short and continues 1 to 10 min, but in subsequent episodes, REM density increases and one episode can be as long as 25 minutes [1, 11].

During REM sleep while neocortex has low amplitude, hippocampus has high voltage theta waves [12]. REM sleep subdivides into two states: phasic and tonic (Figure 1.4). Tonic features include desynchronized EEG, muscle atonia, sleep related erections, sawtooth theta waves, constricted pupils and inhibition of thermoregulation. In this state, penile erections in men and clitoris enlargement in women are tended to be seen. Pupil size is constricted due to parasymphathetic dominance [11]. During REM sleep, thermoregulation is inhibited and humans get into a very rare poikilotermic state. Hence sweating, shivering and panting ability is also reduced. However, during some phasic state of REM sleep, sweating can be seen to decrease body temperature for a brief moment [13].

REM sleep is also an episode where most vivid and illogical dreams have been seen. Roughly 80% of individual's whose woken up during REM episode can describe what they were dreaming about. Loss of muscle tone is considered to be developed to prevent "acting out" during dreaming. Thus, the danger of getting hurt or hurting somebody can be avoided. This mechanism is regulated by brainstem inhibitory centers, such as the midbrain, pontine and medial medullary reticular formations. Muscle activity is repressed by chemically activation of these regions [14]. Subsequently, nearly absent or quiet muscle activity occurs as it can be seen from EMG results. EEG desynchronization of tonic state is achieved by REM-on cholinergic neurons and this desynchronization results with low voltage fast pattern in EEG. The signal for desynchronized EEG pattern also comes from brainstem as well as signal for muscle atonia [15].
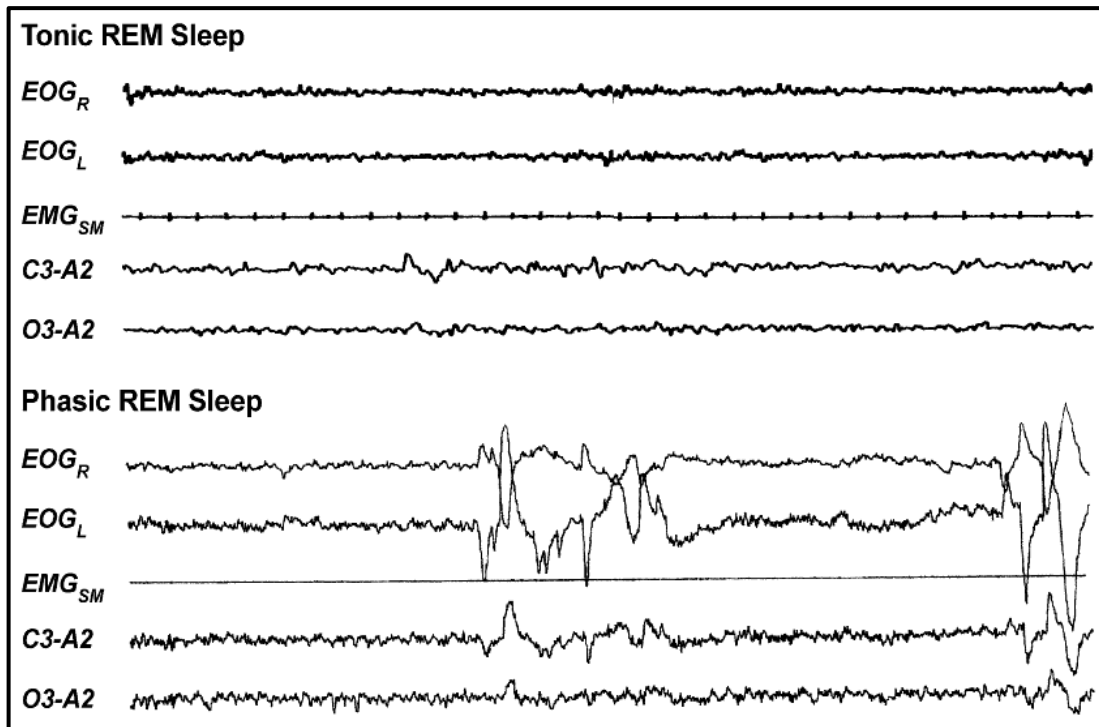
Figure 1. 4 Polysomnographic (EEG-EOG-EMG) tracing of tonic and phasic REM sleep. Each panel shows a 30-second tracing. EOG_R, right electrooculogram; EOG_L, left electrooculogram; EMG_{SM}, submentalis electromyogram; C3-A2, monopolar central electroencephalogram; O3-A2 occipital electroencephalogram [6].

Sawtooth waves are idetified with their triangular shape and 2 to 6 Hz frequency with a high voltage (20 to 100 µV) easy to detect, however these special theta waves can hardly be detected. This pattern can only be seen REM sleep and near central scalp area [11, 16, 17].

Phasic state of REM sleep consists of ponto-geniculo-occipital (PGO) spikes, middle ear muscle activation (MEMA), rapid eye movements, muscular twitches, and irregularities in respiratory and cardiovascular system [11, 18]. Even though, nearly all muscles (except respiratory muscles) are temporarily paralysed during REM sleep, some exceptions can be seen at the phasic state. The muscle jerks can usually be seen in facial muscles and its extremities. These spasms generally are triggered by caudal pontine reticular nucleus and nucleus gigantocellularis [13, 19].

Ponto-geniculo-occipital (PGO) waves are as its name indicated originate from neuronal firing of pons by electrical signal and afterwards this signal project to lateral geniculate nucleus and visual cortex, respectively [20]. PGO waves generally associate with rapid eye movements. Spikes can be used as onset of REM sleep as they appear a

few seconds before REM sleep starts (Figure 1.5) [21]. Rapid eye movements are the phenomena that give the name to this type of sleep. Rapid eye movements are characterized by saccadic and episodic bursts of eye movements. EOG is used to record and measure this characteristic movements. MEMA is the contraction of middle ear muscles during REM sleep. According to Siegel [12], this mechanism has been developed as a protection to loud external auditory stimuli.

The other physiological changes during REM sleep are increased and irregular heart rate and blood pressure, and respiration compared to NREM. Especially, breathing becomes unsteady and faster compared to NREM sleep. Besides, in some cases brief intervals of respiration can be observed [2].
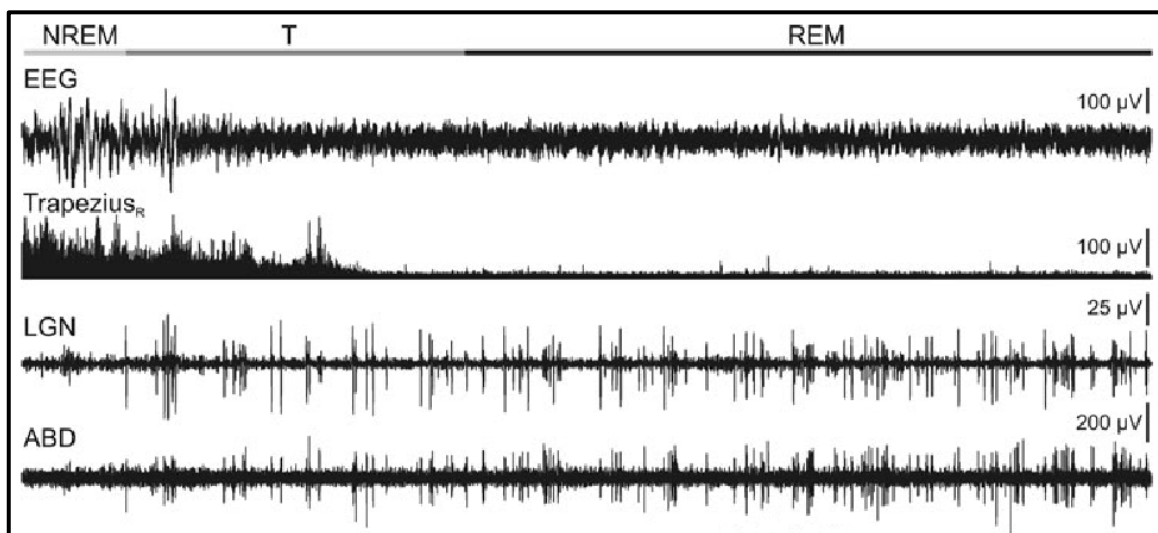
Figure 1. 5 A representative recording of electroencephalography (EEG), right trapezius rectified electromyography (EMG), ponto-geniculo-occipital (PGO) waves at the lateral geniculate (LGN) and abducens (ABD) nuclei. T: transition from NREM sleep to REM sleep [21].

1.1.1.1.3 Circadian Rhythm

Circadian comes from Latin words *circa*, means "about, around" and *dies*, means "day" and it refers a periodic cycle which lasts nearly 24 hours. Sleep-wake cycle, body temperature, hormone secretion, blood pressure, alertness level is controled by inner circadian rhythm. Although mammals have self-regulated endogenous clock, this body clock needs to be adjust to 24 hours by the external cues that are called as "*zeitgebers*", a German word which means "time givers". This process called entrainment. The most powerful zeitgeber is the light. The light/dark cycle regulates

biological cycle through suprachiasmatic nuclei (SCN) which is located anterior of hypothalamus and above optic chiasm [22, 23]. The SCN is entrained by eyes. When light signal hit the retina, photic information is transmitted to SCN cells by the release of glutamate via retinohypothalamic tract (RHT). Furthermore, as an additional pathway this stimulation can be done by retinorecipient intergeniculate leaflet (IGL) via the geniculohypothalamic tract (GHT) [24, 25, 26].
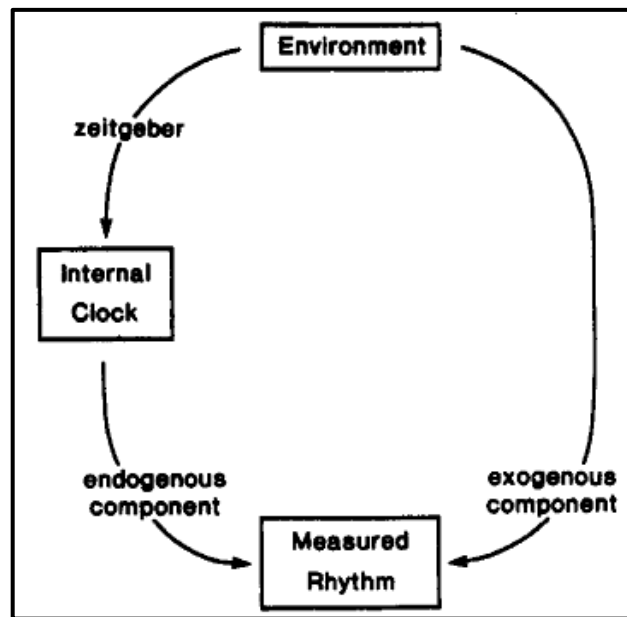
Figure 1. 6 Regulation of circadian rhythm by internal clock, zeitgeber and exogenous components [22].

Melatonin (5-methoxy-N-acetyltryptamine) is an hormone that regulates night cycle of sleep-wake regulation (Figure 1.7) [27]. When the photic information indicates darkness, the inhibiting effect of SCN diminishes. Thus, a neurotransmitter named as norepinephrine releases and this neurotransmitter stimulates pineal gland to secrete melatonin into bloodstream. The increase at the plasma level of melatonin promotes sleep in humans [23, 28]. Plasma of melatonin reaches its peak at 2 to 4 am. At the same time the body temperature starts to decrease due to melatonin reinforcement, and reaches its minimum core temperature roughly at the same time. The SCN has melatonin receptors, therefore rising melatonin level creates a feedback mechanism. Secretion of melatonin drops and the body temperature starts to rise gradually. As a result, the alertness level is increased and arousal state is promoted [29]. Because of

these properties, melatonin has been used to help re-regulation of jet lag, shift work, and circadian rhythm disorders [27, 30].
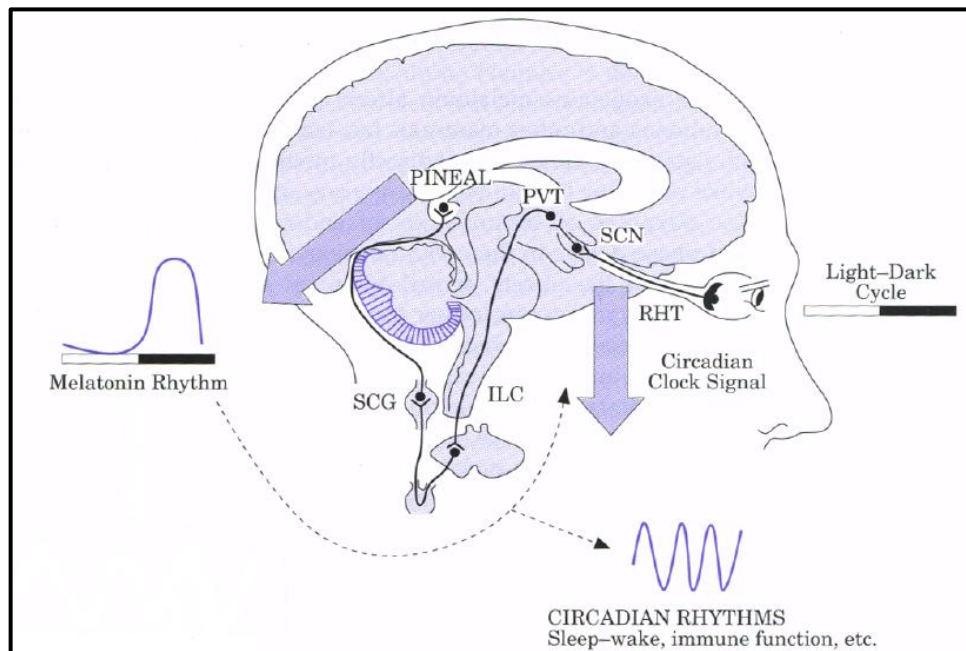
Figure 1. 7 Control mechanism of melatonin secretion through light signal. Adapted from Cardinali and Pévet. SCN: suprachiasmatic nuclei; RHT: retinohypothalamic tract; PVT: paraventricular nuclei; ILC: intermediolateral column of the thoracic chord grey; SCG: superior cervical ganglion; PINEAL: pineal gland [30].

1.1.1.2 Neuroscience of Sleep

1.1.1.2.1   Brain Activity During Sleep

In 1930, Baron Constantin von Economo, a Viennese neurologist, diagnosed a new type of viral encephalitis that affect sleep-wake cycle. With postmortem brain studies, von Economo was able to identify sleep- and wake-promoting centers succesfully. According to these results, while anterior hypothalamus and basal forebrains were associated with sleep regulation, posterior hypothalamus and midbrain were involved with wakefulness [31]. Later in 1949, Moruzzi and Magoun found a transition from sleep-like state to arousal state could be stimulated by excitation of rostral reticular formation in anesthetized cats. Besides, a lesion in the upper brainstem had caused coma or hypersomnolence. This wake state regulation from the brainstem is called ascending reticular activation system (ARAS) [32].

9

Subsequent studies have revealed the dynamic structure of sleep-wake cycle. There are two major pathways in ascending arousal system that regulates wakefulness (Figure 1.8). The first pathway is activated via thalamic neurons that relay information from and to celebral cortex. The signal starts from pedunculopontine and laterodorsal tegmental nucleus (PPT/LDT), a pair of acetylcholine-producing cell groups in the brainstem, and stimulates cortical activation by releasing ACh into thalamus. The PPT/LDT neurons are highly active during wakefulness and REM sleep, and less active during NREM sleep [33, 34]. It is thought PPT/LDT has an important role on REM sleep. It has been reported a lesion in this region leads a significant reduction of REM sleep. And vice versa, when this region is excited, an increase in REM sleep is detected [15, 35].
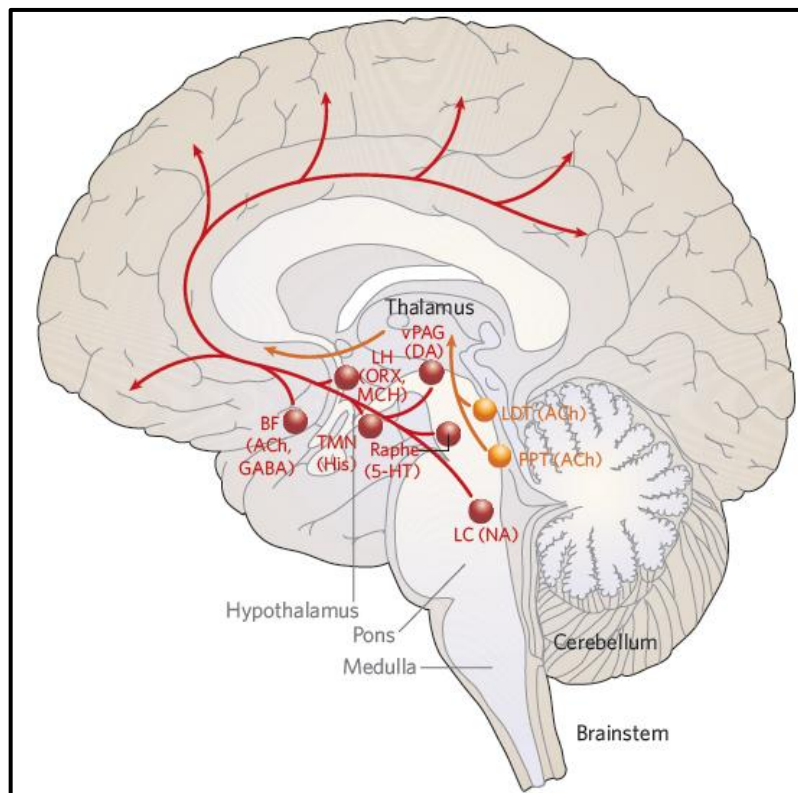
Figure 1. 8 Key components of ascending arousal system. vPAG, ventral periaqueductal gray matter; LDT, laterodorsal tegmental nucleus; PPT, pedunculopontine tegmental nucleus; ACh, acetylcholine; LC, locus coeruleus; TMN, tuberomammillary nucleus; LH, lateral hypothalamus; BF, basal forebrain; GABA, γ-aminobutyric acid; ORX, orexin or hypocretin [33].

The second pathway is the activation of cortex by the neurons in lateral hypothalamus (LH) and basal forebrain (BF). It consists of monoaminergic (brainstem and LH),

dopaminergic (vPAG), histaminergic (TMN), serotoninergic (dorsal and median raphe nuclei), and noradrenergic (LC) cell groups [36]. Melatonin concentrating hormone (MCH) and orexin (or hypocretin) of LH neurons and glutamate or GABA of BF neurons play key roles in REM sleep control. Orexin neurons are only active during wake state and are silent during NREM and REM sleep. The most important thing about orexin is a disease called narcolespy with cataplexy which is seen in the defiency of orexin. As already indicated, MCH and orexin is released from the same place, lateral hypothalamus. However, while orexin neurons are active during wakefulness, MCH neurons are active only during sleep (most active in REM sleep). MCH inhibits orexin-related stimulations and encourage the REM sleep drive [37]. Another REM sleep regulator is GABA or glutamate which is release from sublaterodorsal nucleus (SLD) or LCα. Most of the neurons in SLD fire during REM sleep and this activation causes muscle atonia which characteristic in REM sleep. Hence, lesions in SLD result with disruption of muscle atonia and REM sleep [38].

The histaminargic neurons in tuberomammillary nucleus of posterior hypothalamus stimulates wakefulness. TMN takes the signal from orexin neurons and direct this stimuli to celebral cortex, amygdala and substantia nigra [39].

1.1.1.2.1.1 Ventrolateral Preoptic Nucleus

Sleep-active neurons in VLPO were found by Sherin et al. in 1996 while they were examining c-Fos expression in TMN [34]. VLPO is placed in preoptic area of anterior hypothalamus. It consists of two major nuclei: ventrolateral preoptic nucleus (VLPO) and the extended VLPO. While the sleep active neurons in VLPO has increased firing during NREM sleep, REM sleep is primarily activated by the neurons in extended VLPO [39]. VLPO inhibits major arousal parts (posterior hypothalamus, brainstem, etc.) during sleep state. Conversely, VLPO is down-regulated by these arousal parts (Figure 1.9) [33].

Although, VLPO is not the only sleep-driving system, it has very critical roles. Hence, VLPO lesion effect quality of sleep for months [37].
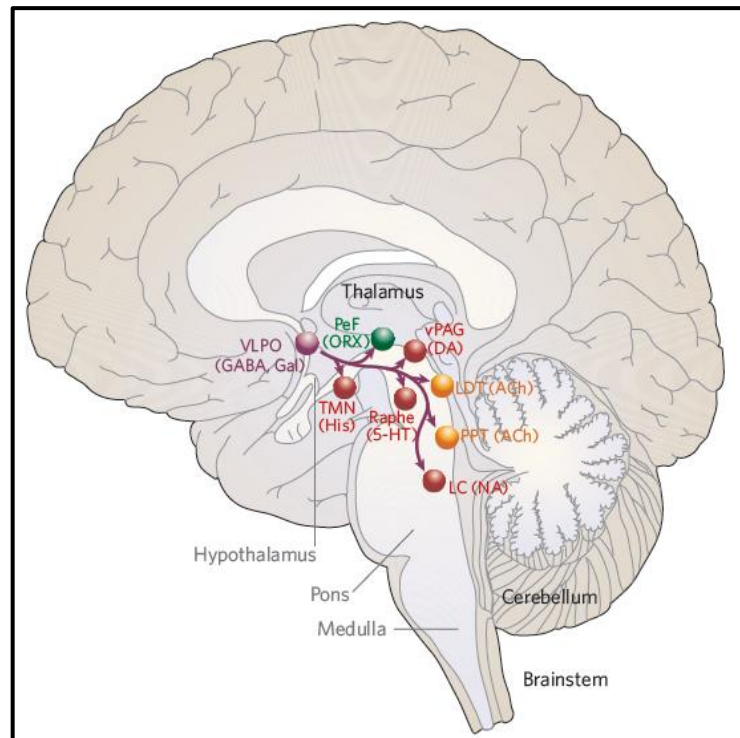
Figure 1. 9 Key projections of the ventrolateral preoptic nucleus (VLPO) to the main components of the ascending arousal system [33].

1.1.1.2.2 Flip-Flop Model

Flip flop is bistable multivibrator that can be made to change state by signals applied to one or more control inputs and will have one or two outputs [40]. Similarly, in wake state, arousal neurotransmitters are released extensively and this situation creates a feedback loop. As a result, VLPO is activated and sleep induction is started (Figure 1.10). Because of flip-flops tend to refrain transitions, the switches usually happen abruptly. This instance can explain why transitions between wakefulness and sleep state are so sharp. Nevertheless, the orexin molecule has a stabilizator effect on this switch and help to avoid unwanted transitions that can be seen in narcolepsy [33].

Although the switch has bistability, if either side is weakened, both side is effected independently of which side is injured. This can be seen clearly from the animals with the VLPO lesion. In consequence, NREM and REM sleep is reduced nearly 50% of sleep time and also, animals wake up often during sleep cycle. Likewise, this situation can be seen older adults, elders lose some of their VLPO neurons along with the age. Eventually, it results in shorter amount of sleep and highly disrupted sleep pattern [36].
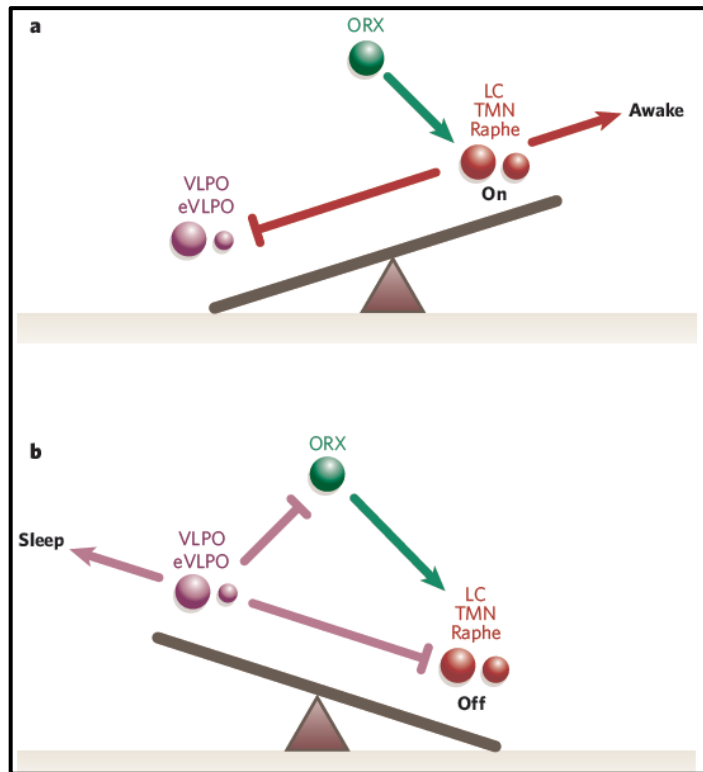
Figure 1. 10 Diagram of the flip-flop switch model. (**a**) Representative figure for awake state according to flip-flop model. When arousal-active regions are active, the feedback loop repressed sleep-active regions. (**b**) Representative figure for sleep state according to flip-flop model. When sleep-active regions are active, the feedback loop repressed wake-active regions [33].

1.1.2 Usage of G Protein-Coupled Receptors as a Neuronal Activity Control Method

A tool that can selectively activate or inhibit neuronal activity *in vivo* is extremely important for mammalian brain function studies. Heretofore, many methods have been developed to accomplish this *in vivo* approach. One of most popular approaches is manipulated G protein-coupled receptors (GPCR). GPCR family is a very large class of cell surface receptors and they respond a wide variety of ligands [41, 42, 43]. Therefore, to control GPCRs create powerful mechanism over central nervous system (CNS) [44].

AlstR (*Drosophila* allatostatin receptor) is a very well-known selective neuronal silencing method via genetically engineered GPCR. AlstR is an insect GPCR that is activated by allatostatin (AL). Strong points of AlstR are it can inactivate a specific type of cell rapidly and reversibly and do not induce any pathology in the body [45]. However, its ligand can not cross blood-brain barrier. As a result, an infusion to brain is

necessary for CNS studies [46]. Also, AlstR can only be used to silence target cell type [47]. Another approach that based on manipulated GPCR signaling pathways is RASSLs (Receptors Activated Solely by Synthetic Ligands). In this approach, GPCRs are mutated to reduce affection to natural ligand without affecting affinity of exogenous small drug-like molecule [43]. Generally, small synthetic molecules are selected as exogenous agonists [44, 47, 48, 49]. RASSLs are usually used together with Tet-Off system to be able to control timing of gene expression. However, it is unknown whether the selected ligands have affinities to other receptors or not and mostly they are pharmocologically active. Another problem is engineered receptors can show pathologic phenotypes. Besides, it has been shown that RASSLs are displayed basal signalling in the absence of synthetic ligand in certain tisues [44, 48, 49].

Another method that have been used commonly is second generation RASSLs or DREADDs (Designer Receptors Exclusively Activated by Designer Drug). This approach, like first-generation RASSLs, aims to adapt GPCRs in a way that the receptors will interact with exogenous ligand more than endogenous ligand. To improve weakness of RASSLs, Armbruster et al. [41] used a muscarinic receptor family and this GPCR family is evolved as it can be activated by a molecule called CNO (clozapine-N-oxide) but not by its natural substrate acetylcholine (ACh). The reasons for the choice of CNO are (1) clozapine (parent compound of CNO) has a high affinity to this receptor family, (2) CNO can cross blood brain barrier and bioavailable in rodents and humans, and (3) CNO is a pharmacologically inert agonist [41, 47]. Affinity of muscarinic subtype 3 (M3) DREADD to natural ligand is reduced via directed molecular evolution approach (Figure 1.11). However interestingly, CNO affinity is sligthly affected by these mutation in M3 receptor (its affinity is increased insignificantly) [41]. Furthermore, DREADD expression do not cause any pathologic effect in the body [47]. Also, GPCRs have different α subunits ($G_{\alpha i}$, $G_{\alpha s}$, $G_{\alpha q}$, $G_{\alpha 12}$) that can be used for different approaches (for example, while Gi-coupled receptors use for silencing neural activity, Gq-coupled receptors activate neurons) [44, 47].
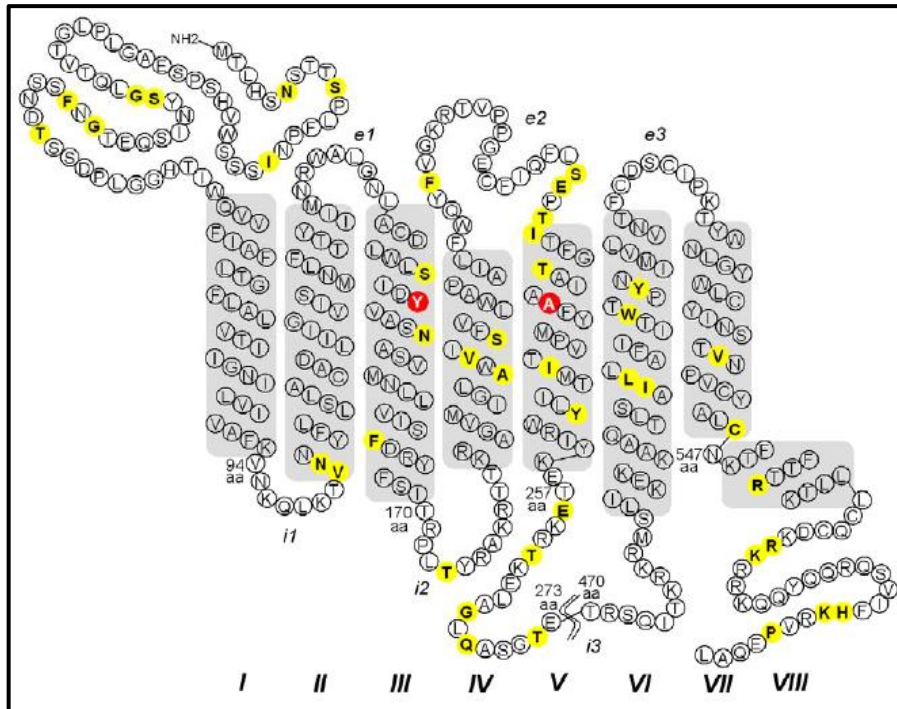
Figure 1. 11 Diagram of M3 DREADD with residues mutated to be sensitive to CNO but not ACh. Red residues were mutated in genetically engineered GPCR. Helixes are marked as gray and image is based on full-length rat M3 receptor [41].

1.1.3 cfos Promoter Linked Tet-Off System

Immediate early gene (IEG) products are generally used as marker for cellular activity which is induced after a stimuli. c-Fos is a member of Fos protein family and a product of an IEG which is named *cfos*. Like many of IEG products, expression of *cfos* is also used to investigate neuronal activity. Under basal conditions, most neurons show low level or none *cfos* expression [50, 51]. Induction of *cfos* is fast and transient and its product has relatively short half-life [51].

Garner et al. [52] used this feature of *cfos* and introduced *cfos*-based transgenic approach with hM3Dq [human muscarinic subtype 3 (hM3) G_q-coupled DREADD] receptor. They used double transgenic hM3Dq[fos] mice in which the control of hM3Dq receptor is depended on neural activity by cfos promoter-driven tTA transgene (Figure 1.12 A). After stimulation, cfos promoter will drive tTA and in the absence of doxycycline (Dox), tTA will activate tetO promoter. The second transgene can only express hM3Dq receptor when tetO is activated by binding of tTA [52]. The power of this method is based on the product of the interest gene is controlled by neuronal activity and only the neurons that fired strong enough can drive the Tet-Off system.

Besides, the time of induction can be controlled by Dox administration [53]. Also, following activation of hM3Dq transgene, hM3Dq receptors can be reactivated artificially by CNO administration in the animal [52] (Figure 1.12 B).
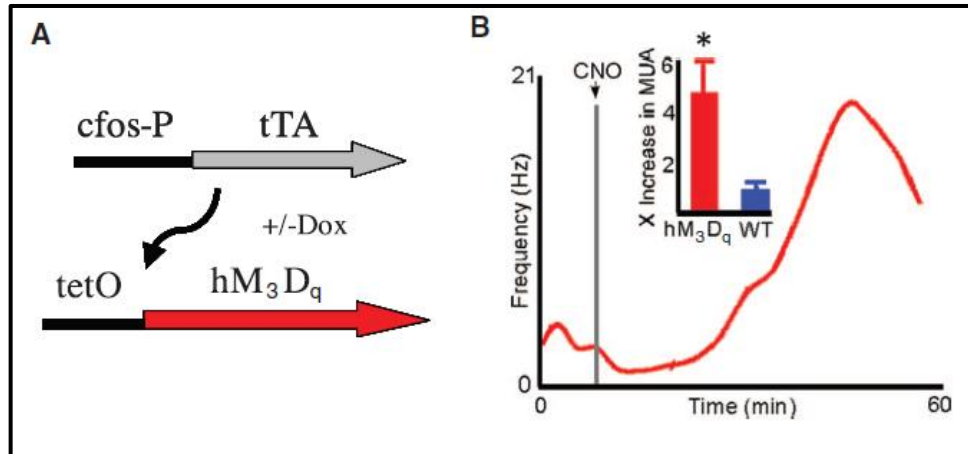
Figure 1. 12 Illustration of the hM3Dq transgene activation and neural activity induced by CNO. (**A**) Diagram of hM3Dq transgene activation under the control of Dox. (**B**) Neural activity induced by CNO in double transgenic hM3Dq[fos] mice. Red curve shows multi-unit activity (MUA) recorded from dorsal CA1 of an anesthetized hM3Dq[fos] mouse over time (*P < 0.01). Adapted from Garner et al. [52].

1.2 Objective of Thesis

The main aim of this study is to understand how we sleep. For this purpose, the mechanism described by Garner et al. [52] to use cfos promoter-driven tTA to control expression of hM3Dq transgene to study memory formation was used to explain sleep promotion in the present study. Similar to Garner et al. [52] first objective of this thesis was preparation of two binary switch mechanisms; (1) cfos promoter-driven tTA and tetO-linked hM3Dq [human muscarinic subtype 3 (hM3) Gq-coupled DREADD] system. (2) cfos promoter-driven tTA and tetO-linked hM4Di [human muscarinic subtype 4 (hM4) Gi-coupled DREADD] system. These plasmids are packaged in AAV vectors and injected in ventrolateral preoptic nucleus (VLPO; sleep active brain area) of mice to test flip-flop model (a model to explain switches between wakefulness and sleep). Present study aims to have a better understanding of sleep promotion and neural mechanism of sleep.

1.3 Hypothesis

The research will be built around the hypotheses are listed below:

a. If we stop Dox administration, both hM3Dq mice and hM4Di mice should be able to express DREADDs in VLPO area.

b. hM3Dq mice injected with CNO while they are awake, animals should go to sleep.

c. hM4Di mice injected with CNO while they are sleeping, animals should wake up.

MATERIAL AND METHODS

2.1 Materials

2.1.1   Chemicals, Enzymes and Kits

GoTaq® Green Master Mix was supplied from Promega (#Cat. No: M7113). Green mix is a ready-to-use solution that contains *Taq* DNA polymerase, dNTP, $MgCl_2$ and reaction buffers at optimal concentrations. All restriction enzymes and their buffers were provided from NEB.

MinElute® Gel Extraction Kit was used from QIAgen (#Cat. No: 28604), High Pure PCR Product Purification Kit from ROCHE (#Cat. No: 11732668001) and GenElute^{TM} Plasmid Miniprep Kit from SIGMA (#Cat. No: PLN350). Quick LigationTM Kit was used from NEB (#Cat. No: M2200S). The kit consists of Quick T4 DNA Ligase (Recombinant) and 2x Quick Ligation Buffer.

HyperLadder 1 (quantitative DNA range in basepairs: 10037, 8000, 6000, 5000, 4000, 3000, 2500, 2000, 1500/1517, 1000, 800, 600, 400, 200) was purchased from Bioline (#Cat. No: BIO-33053). Protein Ladder (10-250 kDa) [molecular weight range in kDa (kilodalton): 250, 150, 100, 80, 60, 50, 40, 30, 25, 20, 15, 10] was supplied from NEB (#Cat. No: P7703S).

Sigma Water was supplied by SIGMA (#Cat. No: W4502), autoclaved and stored at room temperature. SYBR® Safe was provided by Invitrogen (#Cat. No: S33102). Benzonase® nuclease was used from SIGMA (#Cat. No: E1014-25KU).

VectaShield® mounting medium with DAPI was purchased from Vector Laboratories (#Cat. No: H-1200). Fast Green FCF solution (green dye) was supplied from Electron Microscopy Sciences (#Cat. No: 26364-05). SOC Medium was used from NEB (#Cat. No: B9020S).

Gel loading buffer was supplied from Bioline (#Cat. No: BIO-37070) and 2x Sample Buffer with Laemmli was used from SIGMA (#Cat. No: S3401). Dulbecco's modified Eagle medium (DMEM) was used from SIGMA (#Cat. No: D6546). XL1-Blue Supercompetent Cells were purchased from Agilent Technologies (#Cat. No: 200236).

Dox diet was supplied from Harlan (#Cat. No: TD120240).

All other chemicals are purchased from SIGMA, Bioline, Allergan and NEB.

Primers were ordered from SIGMA and sequencing was done at Eurofins.

2.1.2 Antibodies

cFos monoclonal antibody (Santa Cruz Biotechnology, #Cat. No: sc-253)

Alexa Flour 488 goat anti-rabbit IgG (H+L) (Molecular Probes®, #Cat. No: A11034)

Alexa Flour® 594 goat anti-mouse IgG (H+L) (Molecular Probes®, #Cat. No: A11005)

Anti-mCherry monoclonal antibody (Living Colours® mCherry, Clontech, #Cat. No: 632543)

2.1.3 Equipments Used in the Experiments

Stereotaxic instrument (Leica Biosystems)

White Perspex floor (Med Associates)

Upright flourescent microscope (Nikon)

Thermal cycler (Peqlab)

Nanodrop 1000 Spectrophotometer (Thermo Scentific)

Incubator (Heraeus)

Distilled water machine (ONDEO)

pH meter (Radiometer Copenhagen)

Autoclave (Prestige Medical)

Gel imaging system (KODAK EDAS 290)

Centrifugal Filter Concentrator (Millipore)

Heparin Column (SIGMA)

Cell Culture Flasks (Greiner Bio-One)

Heat block (TECHINE)

Ultramicropump (World Precision Instruments)

2.1.4   AAV Vectors and AAV-Helper Plasmids

cfos-htTA plasmid (Figure 2.1) was packaged in AAV to inject into mouse brain. Transformation and isolation step of this plasmid were made by technician. pTRE taulacZ::tTAH100Y (Figure 2.2) construct was used to acquire tetO promoter sequence, and hSyn promoter in pAAV-hSyn-double floxed-hM3D-mCherry (Figure 2.3) and pAAV-hSyn-DIO-hM4Di-mCherry (Figure 2.4) were replaced by tetO promoter.
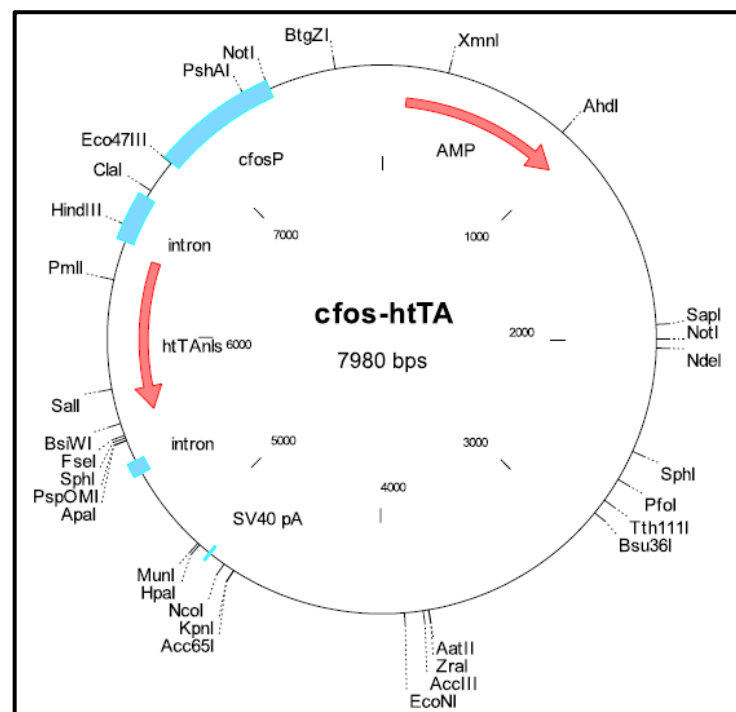
Figure 2. 1 Construct of cfos-htTA (Addgene, Plasmid #34856).
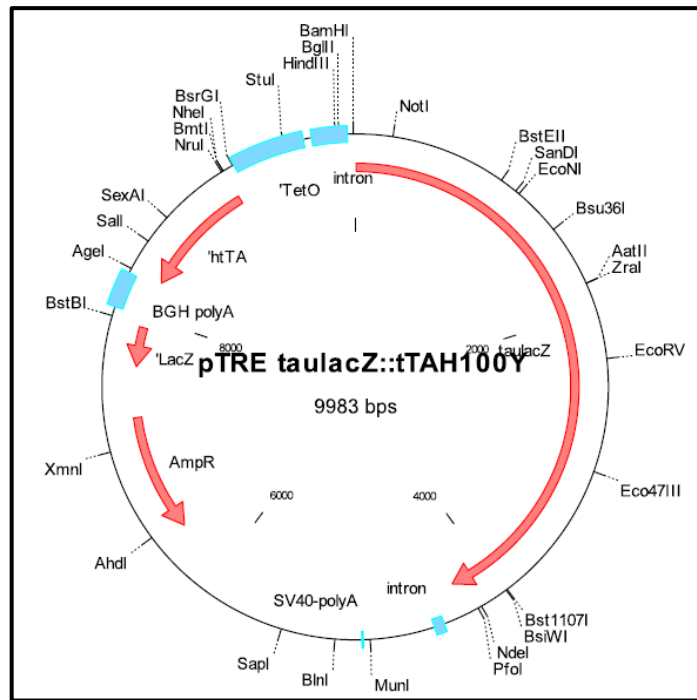
Figure 2. 2 Construct of pTRE taulacZ::tTAH100Y (Addgene, Plasmid #34927).
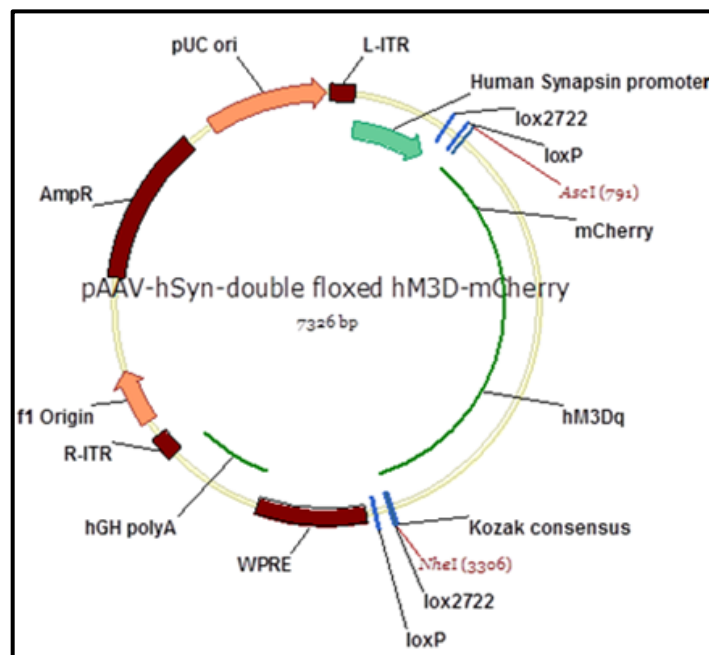
Figure 2. 3 Construct of pAAV-hSyn-double floxed-hM3D-mCherry. hSyn-mCherry-hM3Dq plasmid is a gift from Bryan L. Roth (University of North Carolina).
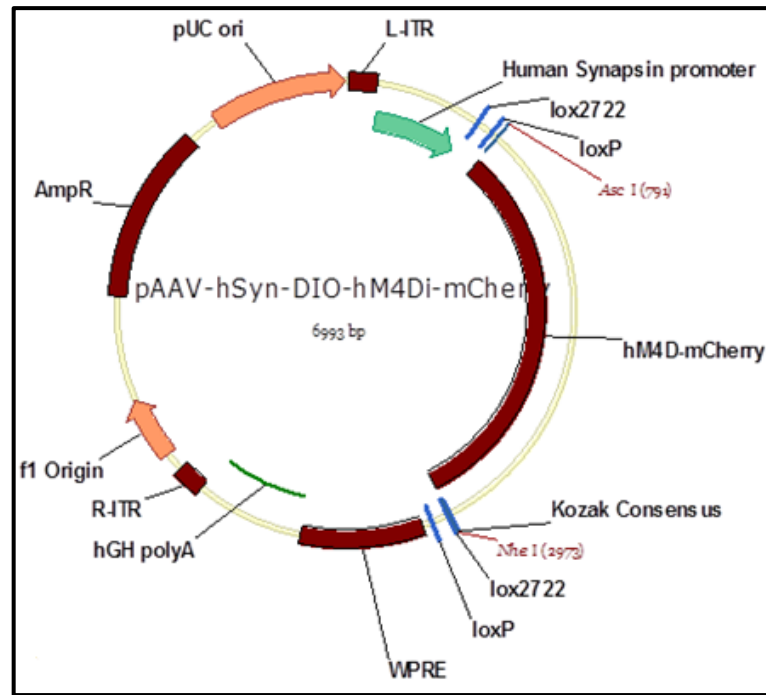
Figure 2. 4 Construct of pAAV-hSyn-DIO-hM4Di-mCherry. hSyn-mCherry-hM4Di plasmid is a gift from Bryan L. Roth (University of North Carolina).

Other plasmids that have been used during experiments are:

− pFΔ6 (adenoviral helper plasmid)

− pH21 (contains an AAV2 *rep* and an AAV1 *cap* gene)

− pRV1 (*cap* and *rep* genes for AAV serotype 2)

2.1.5   Bacteriological Growth Media and Solutions

LB Broth (300 mL) (LB Broth, SIGMA, #Cat. No: L3022)

LB Broth   6 g

MilliQ Water   300 mL

Mixed well and autoclaved. After it was cooled to 50°C, 300 μL ampicillin (amp) was added to solution.

LB Agar

LB Agar   14 g

MilliQ Water   400 mL

Mixed well and autoclaved. After it was cooled to 50$^{\text{o}}$C, 800 µL ampicillin was added to solution. LB/amp agar was poured into petri dishes.

2.1.6 Stock Solutions and Buffers

All solutions and buffers were prepared with MilliQ water or ddH$_2$O unless stated otherwise.

50x TAE buffer (1 L) (Trizma® Base, SIGMA, #Cat. No: T1503)

Trizma® Base	242 g
Acetic Acid	57.1 mL
0.5 M EDTA (pH 8.0)	100 mL

Diluted to 1x TAE with ddH$_2$O before usage.

2.5M CaCl$_2$ (100 mL)

CaCl$_2$.2H$_2$O	36.76 g

2x HEPES Buffered Saline (2x HeBS, pH 7.05, 500 mL)

50 mM HEPES	5.957 g
280 mM NaCl	8.182 g
1.5 mM Na$_2$HPO$_4$	0.1065 g

Filtered and stored in aliquots at -20$^{\text{o}}$C.

1x Phosphate Buffered Saline (PBS) (400 mL) (Phosphate Buffered Saline, SIGMA, #Cat. No: P4417)

2 tablets were dissolved in 400 mL ddH$_2$O.

Autoclaved and stored at room temperature.

2M NaCl Stock (100 mL) (Sodium chloride, SIGMA, #Cat. No: 31434)

NaCl	11.696 g

Filter sterilized and stored at 4$^{\text{o}}$C.

1M Tris Stock (pH8.0, 50 mL)

Trizma® Base   6.057 g

Resuspention Solution (250 mL)

150 mM NaCl   18.75 mL of 2M NaCl Stock

20 mM Tris (pH8.0)   5 mL of 1M Tris Stock

Autoclaved and stored at 4°C.

Sodium Deoxycholate Solution (5 mL) (Sodium deoxycholate, SIGMA, #Cat. No: D6750)

0.5 g sodium deoxycholate

Prepared before usage.

200 mM NaCl, 20mM Tris pH 8.0 (25 mL)

1 M NaCl (filtered)   5 mL

1 M Tris (pH8.0) (filtered)   500 µL

Stored at 4°C.

300 mM NaCl, 20mM Tris pH 8.0 (25 mL)

1 M NaCl (filtered)   7.5 mL

1 M Tris (pH8.0) (filtered)   500 µL

Stored at 4°C.

400 mM NaCl, 20mM Tris pH 8.0 (25 mL)

1 M NaCl (filtered)   10 mL

1 M Tris (pH8.0) (filtered)   500 µL

Stored at 4°C.

500 mM NaCl, 20mM Tris pH 8.0 (25 mL)

1 M NaCl (filtered)   12.5 mL

1 M Tris (pH8.0) (filtered)   500 μL

Stored at 4°C.

1M NaCl, 20mM Tris pH 8.0 (25 mL)

1 M NaCl (filtered)   25 mL

1 M Tris (pH8.0) (filtered)   500 μL

Stored at 4°C.

2M NaCl, 20mM Tris pH 8.0 (25 mL)

2 M NaCl (filtered)   25 mL

1 M Tris (pH8.0) (filtered)   500 μL

Stored at 4°C.

1% VIRKON (1 L)

VIRKON   10 g

0.9% Saline Stock (100 mL)

NaCl   0.9 g

Autoclaved and stored at 4°C.

20% Ethanol (50 mL) (Ethyl alcohol 200 proof (absolute), SIGMA, #Cat. No: E7023)

Ethanol   10 mL

Stored at 4°C.

30% Sucrose Solution (100 mL) (Sucrose, SIGMA, #Cat. No: S0389)

30 g sucrose in ddH$_2$O

Doxycycline (Dox) Solution (Doxycycline, SIGMA, #Cat. No: D9891)

Dox   1 g

Sucrose   50 g

Covered with foil to avoid light and stored at 4^oC.

Clozapine-*N*-oxide (CNO) Solution (10 mL) (CNO, SIGMA, #Cat. No: C0832)

CNO   0.5 mg

0.9% Saline   10 mL

4% Paraformaldehyde (PFA) Solution (200 mL) (16% Formaldehyde solution (w/v) methanol free, Thermo Scientific, #Cat. No: 28908)

16% PFA solution   50 mL

1x PBS solution   150 mL

Prepared before usage.

0.4% Triton X-100 in PBS (100 mL) (Triton X-100, SIGMA, #Cat. No: T8787)

Triton X-100   0.4 mL

1xPBS   100 mL

Dissolved and stored at 4^oC.

0.3% PBX Solution (50 mL)

1x PBS   5 mL

ddH$_2$O   44.85 mL

Triton X-100   0.15 mL

2.1.7   Primers

10x primer solutions were diluted to 1x before use in PCR. The restriction sites of restriction enzymes are shown in red below.

Primers for amplification of TetO promoter:

TetO Mlu F: 5'-CACACGCGTCACCTTAATATGCGAAGTG

Tm=74.4^{o}C

TetO Sal R: 5'-GGCCGTCGACGACAGCGAATTCTAGAATC

Tm=77.4^{o}C

Primer for amplification of mCherry-hM3Dq sequence:

hM3 NheI F: 5'-CGAAGGTTATGGCTAGCCTTACTTGTACAGCTCG

Tm=69.4^{o}C

hM3 AscI R: 5'-CTTTATACGAAGTTATGGGCGCGCCACCATGAC

Tm=79.1^{o}C

Primer for amplification of mCherry-hM4Di sequence:

pAAV hM4D mCherry F: 5'-GCGCGGGCTAGCCTTACTTGTACAGCTCGTCCTA

Tm=81.5^{o}C

pAAV hM4D mCherry R: 5'-GAGAGGCGCGCCGCCACCATGGCCAACTTCACC

Tm=90.4^{o}C

2.2 Methods

2.2.1 Preparing the Binary Switch Constract

2.2.1.1 Polymerase Chain Reaction

PCR to amplify tetO promoter (Table 2.1) was begun with first denaturation step at 95°C for 2 minutes. First cycle was constituted denaturation at 95°C for 45 seconds, annealing 58°C for 45 seconds and elongation 72°C for 1 min 30 seconds. The reaction were repeated itself for 30 cycles. After last cycle, PCR were ended with last elongation step at 72°C for 10 minutes.

Table 2. 1 PCR components to amplify tetO promoter from pTRE taulacZ::tTAH100Y.

2x Green Mix	25 μL
ddH$_2$O	22 μL
1x Primer Mix (TetO Mlu F and TetO Sal R)	2.5 μL
pTRE taulacZ::tTAH100Y	0.5 μL
Total	**50 μL**

PCR to amplify mCherry-hM3Dq sequence (Table 2.2) was begun with first denaturation step at 95°C for 2 minutes. First cycle was constituted denaturation at 95°C for 45 seconds, annealing 58°C for 45 seconds and elongation 72°C for 1 minute and 45 seconds. The reaction were repeated itself for 35 cycles. After last cycle, PCR were ended with last elongation step at 72°C for 10 minutes.

Table 2. 2 PCR components to amplify mCherry-hM3Dq sequence from pAAV-hSyn-double floxed-hM3D-mCherry.

2x Green Mix	25 μL
ddH$_2$O	22 μL
1x Primer Mix (hM4 NheI F and hM4 AscI R)	2.5 μL
pAAV-hSyn-double floxed-hM3D-mCherry	0.5 μL
Total	**50 μL**

PCR to amplify mCherry-hM4Di sequence (Table 2.3) was begun with first denaturation step at 95°C for 2 minutes. First cycle was consisted of denaturation at 95°C for 45 seconds, annealing 58°C for 45 seconds and elongation 72°C for 1 minute and 45 seconds. The reaction were repeated itself for 35 cycles. After last cycle, PCR were ended with last elongation step at 72°C for 10 minutes.

Table 2. 3 PCR components to amplify mCherry-hM4Di sequence from pAAV-hSyn-DIO-hM4Di-mCherry.

2x Green Mix	25 μL
ddH$_2$O	22 μL
1x Primer Mix (hM3 NheI F and hM3 AscI R)	2.5 μL
pAAV-hSyn-DIO-hM4Di-mCherry	0.5 μL
Total	**50 μL**

2.2.1.1.1 Purification of DNA after PCR

High Pure PCR Product Purification Kit was used for purification after PCR and digestion.

2.2.1.2 Agarose Gel Electrophoresis

0.8% agarose gel prepared with the mixture of 0.8 g agarose, 100 mL 1x TAE buffer and 2 µL SYBR® Safe. 0.8 g agarose and 100 mL 1x TAE buffer were microwaved for 1 minute and when mixture was cooled down to 40°C, SYBR® Safe was added into 25 mL agarose gel. Gel casting tray was placed into tank and secured it with two dams. The comb was placed and gel was poured. After gel was cooled to room temperature, the dams were removed. The gel tank filled with 1x TAE buffer and the comb was removed. Samples and ladder was loadded. The gel was run at 80 to 85 volts (V) for 35 to 60 minutes.

2.2.1.3 Purification from Agarose Gel

The gel was checked with KODAK Electrophoresis Documentation and Analysis System 290. DNA fragments at the size of the target sequence was cut off and extracted using MinElute® Gel Extraction Kit.

2.2.1.4 Digestion and Ligation Reactions

All digestion and ligation steps are explained in results to avoid any probable confusion.

2.2.1.5 Transformation and Isolation of Recombinant Plasmid DNA

XL1-Blue supercompetent cells were taken out of -80°C freezer and thawed on ice. 5 µL ligation product was put in 1.5 mL eppendorf tube and placed on ice. 50 µL XL1-Blue supercompetent cells were added to eppendorf tube and left on ice for 30 minutes. After 30 minutes, eppendorf tube was placed on heat block at 42°C for 45 seconds. Afterwards, the tube was put on ice quickly for another 2 minutes. 450 µL SOC medium was added and the eppendorf tube was placed in an incubater at 37°C for 30 min with

rotation. Later, 200 μL of transformation solution were plated onto each LB/amp agar plates. Plates were incubated at 37°C for 14 hours.

After 14 hours, plates were checked for the bacterial colonies. Colonies were picked and incubated in 15 to 20 mL LB media with ampicillin at 37°C overnight with rotation at 220 rpm. DNA was purified and isolated with GenElute^{TM} Plasmid Miniprep Kit. All solutions and columns were provided from the kit. All spins were performed at 12000 x g and room temperature, unless stated otherwise.

Overnight cultures were centrifuged at 4100 x g for 6 minutes and supernatant was discarded. 200 μL Resuspention Solution were added to tubes and cell pellets were resuspended with the help of vortex. Resuspended solution were transfered 2 mL eppondorf tubes and 200 μL Lysis Solution was added. The tubes were inverted to mix and waited for about 5 minutes until the lysate get a clear view. Afterwards, 350 μL Neutralization Solution were added and mixed with invertion. Tubes were spinned at 13000 x g for 10 minutes.

Meanwhile, GenElute column was placed in a collection tube and 500 μL Column Preparation Solution were added into the column. Tubes were spinned for 1 minute and flow-through were discarded. After the columns were prepared, the clear lysate were transfered into the columns. Tubes were spinned for 30 seconds and flow-through were discarded. 750 μL Wash Solution were added to columns and the tubes were spinned for 30 seconds. Flow-through were discarded and tubes were spin-dried for 1 minute. Before elution step, columns were placed into new collection tubes and 50 μL ddH2O were added. Tubes were spinned for 1 minute and flow-through were stored at -20°C.

2.2.1.6 Control of Designed Structure of Recombinant Plasmid DNA

AAV vectors double-digested with proper restriction enzymes to confirm their last structure and a gel was run with the digestion sample. Later, the results was verified with sequencing Eurofins.

2.2.2 AAV Virus Production

2.2.2.1 Transfection

Whole procedure was carried out in Class II tissue culture hood. The hood was sterilezed with 70% ethanol before and after all procedures. The transfection was performed with human embryonic kidney 293 (Hek293) cells in five 175cm^2 flasks. The cells was under passage 30 and about 70% confluence. Before transfection sterile water, 2.5M $CaCl_2$ and 2x HeBS were warmed up to room temperature. Transfection mixture was prepared with 62.5 µg AAV plasmid, 125 µg pFΔ6, 31.26 µg pRVI, 31.25 µg pH21 and 1650 µL 2.5M CaCl2, respectively. Transfection mixture was filtered with 0.2 µm syringe filter into a sterile 50 mL falcon tube. 13 mL 2x HeBS were added quickly while vortexing the falcon tube intensely and vortexed for 10-15 more seconds and left for 15 minutes. Afterwards, a clear white precipitate was formed. Five 175 cm^2 flasks were took out of the incubator and put 5 ml of transfection solution to each flask drop by drop. Then gently a horizontal position was provided and swirled [54].

16 hours after transfection, medium was changed with 50 mL of fresh DMEM. DMEM was warmed up beforehand to 37°C. Waste was decontaminated with 1% VIRKON and disposed.

2.2.2.2 Harvesting Cells

60 to 65 hours after transfection, five flasks were taken out of incubator and washed cells with their own medium. Cells were divided each into two 25 mL lots in 50 mL falcon tube. The falcon tubes was centrifuged at 800 x g for 7 minutes at 4°C and supernatant was discarded. Cells were resuspended with 5 mL PBS to each tube. Then, two tubes were integrated into each other and added 10 mL more PBS. Centrifuge step was repeated and supernatant was discarded. 5 mL PBS was added each tube and resuspended. Two tubes were combined into each other and the suspension was divided in the last tube into two, equally. At last step, all cells were collected in two falcon tubes. 10 mL more PBS was added and mixed into each tube. The tubes can be frozen overnight at -20°C before proceeding further. Waste was decontaminated with 1% VIRKON and disposed.

2.2.2.3 Digestion of AAV-Infected Cells

If the tubes were frosted, they should be defrosted at room temperature. The falcon tubes were centrifuged at 800 x g for 7 minutes at 4°C and supernatant was discarded. 25 mL resuspention solution, 1.25 mL sodium deoxycholate solution, and 4.25 µL benzonase endonuclease (final concentration of 50 U/mL), respectively, were added into tubes [54]. The tubes were mixed fully and incubated in a waterbath at 37°C for an hour. After an hour, they were centrifuged at 3000 x g for 15 minutes at 4°C to remove cell debris. Supernatant were poured into new 50 mL falcon tubes. This step should repeat to remove remaining cell debris until a clear supernatant is acquired. The samples can be kept at -20°C until heparin column purification for several weeks. Waste was decontaminated with 1% VIRKON and disposed.

2.2.2.4 Heparin Column Purification

An heparin column purification method had been used to purify AAV1/2 stereotype [54]. Samples were defrosted at room temperature, then centrifuged at 3000 x g for 15 minutes at 4°C to remove debris. At the same time heparin column was setup (Figure 2.5). A 60 mL disposable syringe was attached to the column via peristaltic pump and a beaker was placed to collect flowthrough. Pump was set at 1 mL/min flow rate. Before the attachment of the column, the tube was cleaned with 15 mL resuspension solution. The column was adjoined and loaded 10 mL more resuspension solution to wash heparin column. Sample was added into syringe. When the sample was almost run out, it was washed with 15 mL resuspension solution. 1 ml 200 mM NaCl, 20 mM Tris, pH 8.0 and 1 ml 300 mM NaCl, 20 mM Tris, pH 8.0, respectively, were added and washed. Flow-through was discarded. The column was placed on top of a sterile 50 mL falcon tube to collect flow-through before adding 400 mM NaCl, 20 mM Tris pH 8.0. The virus was eluted from the column by adding 1.5 mL 400 mM NaCl, 20 mM Tris pH 8.0, and following by 3 mL 500 mM NaCl, 20 mM Tris pH 8.0, lastly 1.5 mL 1M NaCl, 20 mM Tris pH 8.0. Finally column was washed with 10 mL 2M NaCl, 20 mM Tris pH 8.0 and collected 1 mL of this fraction and the column was broken off from falcon tube and detached to beaker again [54].
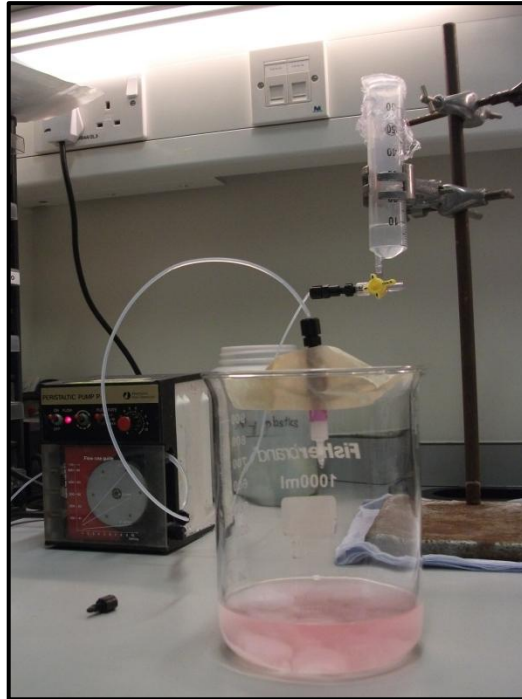
Figure 2. 5 Heparin column setup for virus purification.

The collected sample was put into centrifugal concentrator and spined at 2000 x g for 30 minutes at 4°C. The concentrator was refilled with 3.5 mL 0.9% NaCl solution and centrifuged at 2000 x g for 30 minutes at 4°C again. Centrifugal procedure was proceeded until the volume is concentrated to about 250 μL. The flow-through was discarded into the beaker. Concentrated virus was aliquoted into sterile PCR tubes each of 10 mL and stored at -80°C [54].

Meanwhile, column was washed with 20 mL 20% ethanol and taken off the column. 50 mL 1% VIRKON and 50 mL ddH$_2$O, respectively, were added. The waste was put into beaker and 1% VIRKON was poured. It was labeled as viral decontamination and decontaminated overnight. All the solid waste was put into an autoclave bag and disposed [54].

2.2.3   Animals and Surgery

All animals were male C57/BL6 mice (10 to 12 weeks old). All procedures were carried out under UK Home Office Licensing. Animals were kept under a strict light-dark cycle (lights on at 19:30, lights off at 07:30). Before experiments, a minimum of four days adaptation period to new environment was given to all animals.

2.2.3.1 AAV Injection

Pre-operation animals were administered 0.08 mg/kg subcutaneous buprenorphine as analgesic and anesthesized with 2-2.5% isoflurane in medical O_2 at a flow rate of approximately 0.5 L/min by inhalation and maintained throughout surgery. Anesthesized animals were placed to stereotaxic frame on top of the heat mat and secure their head by ear bolts. Ocular lubricant was applied to eyes of the animals. Injections were done with 1 μL cfos-tTA in AVV and 1 μL tetO-hM3Dq-mCherry in AAV for hM3Dq injection and 1 μL cfos-tTA in AVV and 1 μL tetO-hM4Di-mCherry in AAV for hM4Di injection. Injection mixture was prepared with 20% Mannitol (to increase AAV spread) at a ratio 1:1 with virus mixture (total 2 μL volumes) [55] and added a small amount of green dye to mark the injection site.

A digital mouse brain atlas software used that is linked to the stereotaxic instrument to target of VLPO. Stereotaxic coordinates were based on Franklin and Paxinos's atlas of the mouse brain [56]. Injections were performed with 10 μL Hamilton syringe at a rate of 0.2 to 0.5 μL/min controlled by an ultramicropump. AAVs were injected bilaterally: left injection (Bregma -5.4, ML +0.8, dorsolateral (DL) -3.6), right injection (Bregma -5.4, ML -0.8, DL -3.6) (Figure 2.6). 1 μL injection mixture was injected into each site. The needle was left for 1 to 5 minutes to help diffusion and then retracted. After surgery, animals were removed into recovery cage with homeothermic blanket and given 0.8 mL/200 mL water 2.5% BayTril antimicrobial solution in their water.
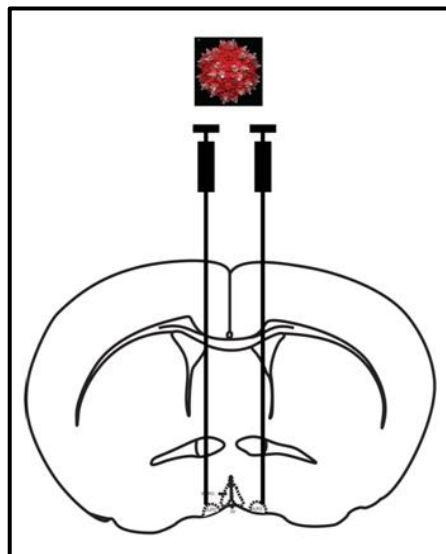
Figure 2. 6 Diagram for AAV vector injection in VLPO area.

34

2.2.3.2 ECoG/EMG Placement and Recordings

Pre-operation animals were administered 0.08 mg/kg subcutaneous buprenorphine as analgesic and anesthesized with 2-2.5% isoflurane in medical O_2 at a flow rate of approximately 0.5 L/min by inhalation and maintained throughout surgery. After AAV injection procedure was completed, the reference-ground ECoG (electrocorticography or intracranial EEG) electrode was implanted into the parietal bone (Bregma -1.5, mediolateral (ML) +1.5), one electrode was placed into the frontal bone (Bregma +1.5, ML -1.5) and another into the interparietal bone located over the cerebellum (Lambda -2.0, ML 0.0) (Figure 2.7 b). The electrodes were secured to the skull with dental cement. For EMG, three Teflon-insulated stainless steel wires (with the distal 3mm exposed) were embedded into the neck muscles just behind the skull. After surgery, animals were removed into recovery cage with homeothermic blanket and given 0.8 mL/200 mL water 2.5% BayTril antimicrobial solution in their water.

The Neurologger 2 that was used for the recordings had seven pins and first pin was used as ground. The first two pin (pin 1 and 2) was soldered at the neurologger and connected to reference electrode to create another ground. Therefore, this soldered-pin named as "2" and used as second reference point as shown in the Figure 2.7 (a).
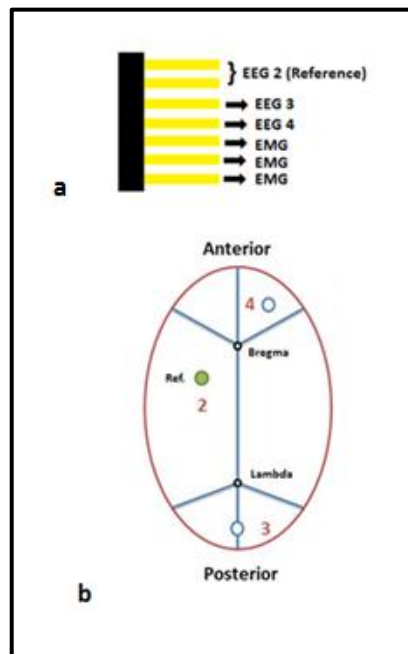
Figure 2. 7 Placement of EEG electrodes and illustration of EEG pins. (**a**) A simplified schematic of neurologger pins. (**b**) Position of ECoG electrodes on skull.

35

Cortical and muscle tone activity were recorded on a 256 MB memory Neurologger 2 device that originally designed to record EEG and EMG activity of flying pigeon [57]. Before performing all recordings, a mock logger was attached to animals to acclimatize animals to neurologger. The data loggers were connected directly to electrode pins to avoid recordings that occurs due to external factors (e.g., mice movements). Neurologer was attached on animal and EEG signals were recorded for 15 minutes. Later to evaluate baseline, saline was injected and signals were continued to record for 30 minutes. Afterwards, EEG recording was completed with 30 minutes for before CNO injection period and 30 minutes for after CNO injection period. An authenticated protocol was used to score all recordings as REM sleep, NREM sleep or wakefulness [58, 59].

2.2.4 Sleep Deprivation Experiments

All CNO injections were carried out as intraperitoneal (IP) injections.

2.2.4.1 Sleep Deprivation Before Immunohistochemistry Tests

2.2.4.1.1 Sleep Deprivation Before Immunohistochemistry with cFos Monoclonal Antibody

After AAV injection, all mice are given 1 mg/mL Dox by drinking or 40 mg/kg Dox by diet for 3 weeks. After 3 weeks, mice were kept awake for 5 hours and then sacrificed (n=2) or allowed to sleep for 2 hours (n=2) and then sacrificed. Brains were sliced and immunohistochemistry (IHC) procedure was applied to brain slices. An upright flourescent microscope was used to monitorize all slices.

2.2.4.1.2 Sleep Deprivation Before Immunohistochemistry with Anti-mCherry Monoclonal Antibody

For first trial of co-injection, we had waited for 3 weeks after injection for virus expression. After 3 weeks, animal was kept awake for 5 hours and allowed to sleep for 2 hours and then sacrificed (n=1). Brain was sliced immunohistochemistry procedure was applied to brain slices. An upright flourescent microscope was used to monitorize all slices.

Following first trial of AAV injection, three sets of mice had been prepared and all mice were given 1 mg/mL Dox by drinking or 40 mg/kg Dox by diet for 3 weeks. After 3 weeks of period, ON DOX mice (n=2) were kept on Dox all the time and after sleep deprivation (SD) of 5 hours and recovery sleep (RS) of 2 hours, they were sacrificed. Dox administration was stopped for OFF DOX+12H mice and OFF DOX+3DAYS mice. Subsequently, OFF DOX+12H mice (n=2) were kept awake for 5 hours and allowed to recover 12 hours and then sacrificed. OFF DOX+3DAYS mice (n=2) were kept awake for 5 hours and kept off Dox 3 more days and then sacrificed. Brains were sliced and immunohistochemistry procedure was applied to brain slices (Figure 2.8). An upright flourescent microscope was used to monitorize all slices.
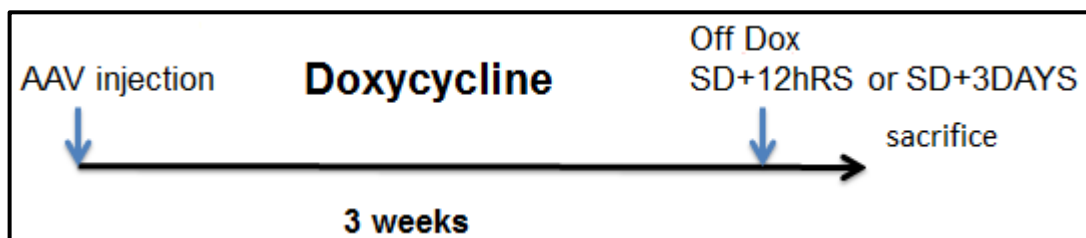
Figure 2. 8 Time schedule for sleep deprivation experiment before immunohistochemistry with anti-mCherry monoclonal antibody.

2.2.4.2 Sleep Deprivation Before Animal Behaviour Test

After AAV injection, animals were kept off Dox for 3 weeks. Before behavior test, they were injected 0.5 mg/kg CNO or 0.9% saline and experiments were performed 30 minutes after injection (Figure 2.9). Saline injection was used as negative control.
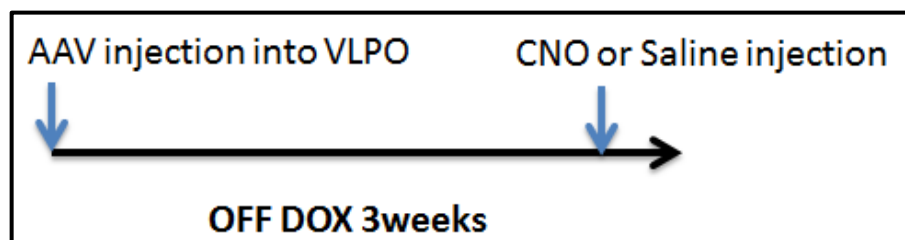
Figure 2. 9 Animal care process before animal behavior test.

Separately, three sets of mice has been prepared to understand effect of Dox administration to behavior test. On Dox mice (n=6) were given Dox all the time. After 5 hours of sleep deprivation, 3 days of recovery period was given. Off Dox 12h mice (n=6) were kept on Dox for 3 weeks. After 3 weeks, Dox administration was stopped

and subsequently 5 hours of sleep deprivation and 12 hours of recovery period was carried out. Off Dox 4 Weeks mice (n=4) were given Dox for 3 weeks and then Dox administration was stopped. Afterwards, 5 hours of sleep deprivation and 4 weeks of recovery period were performed. Following to recovery period, 0.5 mg/kg CNO was injected to each mice and 30 minutes later, locomotor activity test was carried out.

2.2.4.3 Sleep Deprivation Before EEG Recordings

After AAV co-injection, control animal was put on Dox for 3 weeks and test animal was put on Dox for 3 weeks and sleep-deprived for 5 hours. Later, Dox administration was stopped and test mouse was allowed to recover for 12 hours. After 0.5 mg/kg CNO injection, EEG recordings were done.

2.2.5   Animal Behavior Test

2.2.5.1 Locomotor Activity

The locomotor activity test was performed in a 27 cm^2 box with a white Perspex floor in which there are 16 x 16 evenly spaced infrared beams crossing 2 cm above the floor. The mouse was placed in open field to explore for 30 minutes. Med Associates Activity Monitor Version 5 was used to record field activity of mice. Position and movements of animal were calculated by a software that use the record of broken infrared beam data by sampling the position 20 times per second. The software we used computes distance travelled, total time ambulatory and average velocity.

2.2.6   Brain Slice Preparation

2.2.6.1 Perfusion

Following EEG recordings and AAV spreading, mice were anesthesized with 2-2.5% isoflurane in O_2 by inhalation and maintained during surgery. Animal's chest was opened with a sterilized scissors. A blunted needle was placed to the left ventricle of the heart and a small hole was opened at the right ventricle. The animal was perfused with 30 mL of cold PBS at 3 mL/min and afterwards it was replaced with 30 mL of 4% PFA at 3 mL/min. Skull was opened and the brain was removed. Brain was fixed in 4%

PFA for 24 hours followed by 30% sucrose for 24 to 48 hours. The brain was ready to be sliced when it is sunk in 30% sucrose.

2.2.6.2 Brain Slice Method

Microtome was cooled down with dry ice. When it was cold enough to freeze the brain, the fixed brain was positioned (Figure 2.10). After the brain was frozen completely, it was sliced at a thickness of 45 μm. The slices were stored in a cell culture plate that filled with PBS at 4°C until immunohistochemistry procedure was performed.
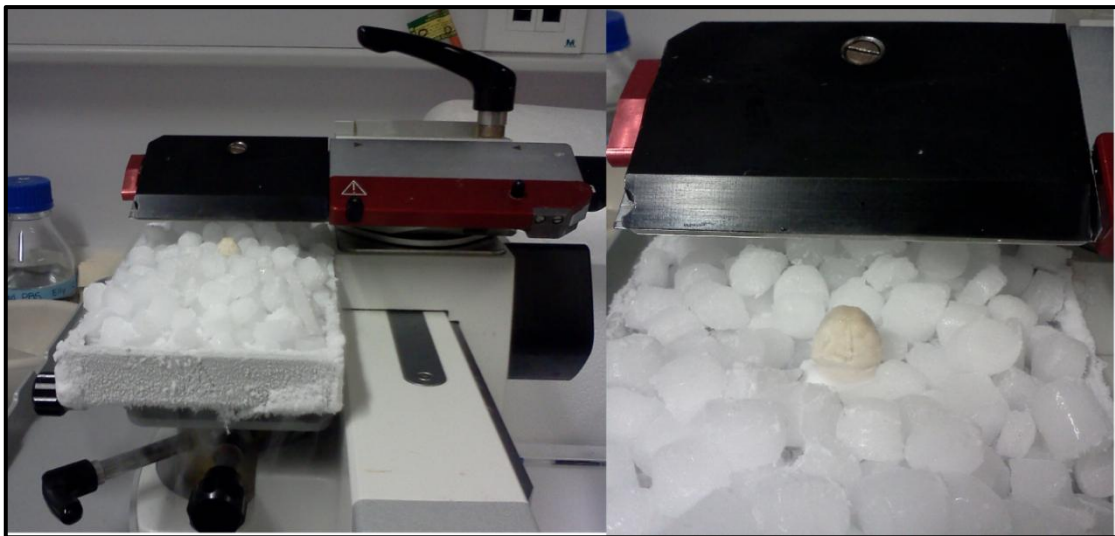
Figure 2. 10 Image of microtome and the process of taking brain tissue slices.

2.2.7   Immunohistochemistry

All procedures were carried out at room temperature with rotation unless stated otherwise.

2.2.7.1 Immunohistochemistry with cFos Monoclonal Antibody

Free-floating sections were washed in PBS three times for 10 minutes and permeabilized in PBS plus 0.4% Triton X-100 for 30 min. 8% normal goat serum (NGS) and 0.2% Triton X-100 in PBS was prepared for the blocking step. Sections were blocked in blocking solution for 1 hour. cFos antibody solution was prepared with 2% NGS in PBS and antibody was added with a ratio 1:10000. Afterwards, sections were incubated with primary antibody for 24 hours at 4°C. After primary antibody

treatment, slices were washed in PBS three times for 10 minutes. Secondary antibody solution was prepared with 1:1000 dilution of goat anti-rabbit antibody in PBS plus 2% NGS. Sections were incubated for 2 hours. Subsequently, slices were washed in PBS three times for 10 minutes. Sections were mounted on microscope slides, embedded in mounting medium and cover-slipped. An upright flourescent microscope was used for imagining.

2.2.7.2 Immunohistochemistry with Anti-mCherry Monoclonal Antibody

Free-floating sections were washed in 0.3% PBX three times for 10 minutes. 8% NGS and 0.2% Triton X-100 in PBS was prepared for the blocking step. Sections were blocked in blocking solution for 1 hour. Anti-mCherry antibody solution was prepared with 2% NGS in PBS and antibody was added with a ratio 1:2000. Afterwards, sections were incubated with primary antibody for 24 hours at 4°C. After primary antibody treatment, slices were washed in 0.3% PBX three times for 10 minutes. Secondary antibody solution was prepared with 1:1000 dilution of goat anti-mouse antibody in PBS plus 2% NGS. Sections were incubated for 2 hours. Subsequently, slices were washed in PBS three times for 10 minutes. Sections were mounted on microscope slides, embedded in mounting medium and cover-slipped. An upright flourescent microscope was used for imagining.

RESULTS AND DISCUSSION

3.1 Binary Genetic Switch Construct in AAV

3.1.1   Preparation of tetO Insert

PCR was conducted to amplify tetO promoter (Figure 3.1). 0.8% agarose gel was prepared and samples were run at 85 V for 59 minutes. The gel was screened and its picture was taken with gel imaging system. Figure 3.2 shows that the band for tetO promoter. After gel electrophoresis, the band for tetO promoter was cut with the help of a surgical blade and purified.
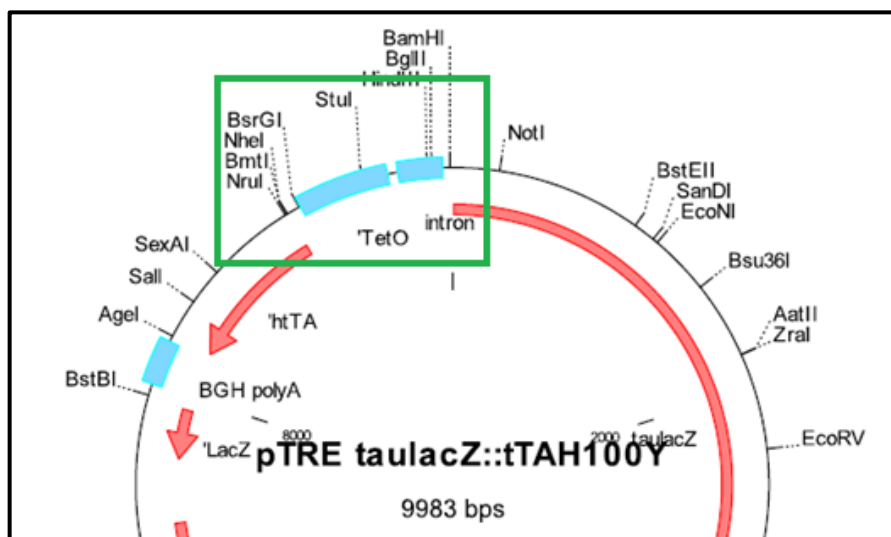
Figure 3. 1 Position of tetO promoter in the construct of pTRE taulacZ::tTAH100Y.
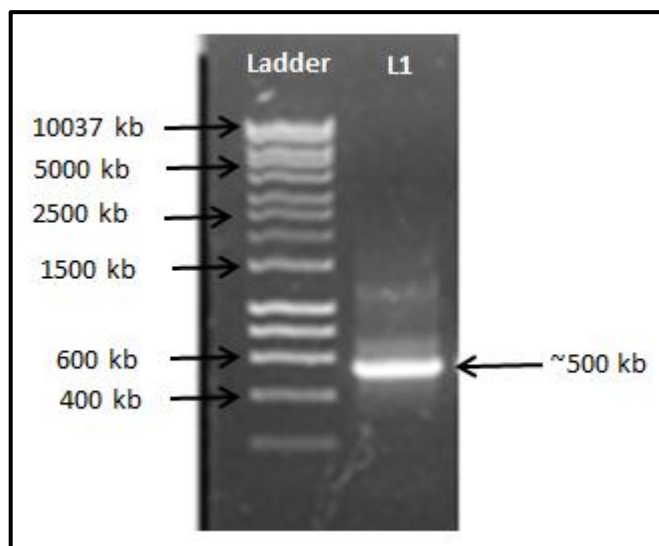
Figure 3. 2 PCR result for amplification of tetO promoter. L1: PCR product.

Purified PCR products were doubled-digested with the restriction enzymes MluI and SalI. Digestion reaction was prepared with the compnents shown in the Table 3.1 and incubated at 37°C for 2 hours. Digestion product was purified with PCR Product Purification Kit to use the tetO promoter after digestion. Regardless of the kit is a PCR Product Purification Kit, the kit aims to remove all enzymes and chemicals. Therefore, it can be also use to purify digestion products.

Table 3. 1 Components of the digest reaction from tetO promoter-PCR product.

tetO promoter	2 µL
ddH$_2$O	5 µL
MluI	1 µL
SalI	1 µL
NEBuffer 3	1 µL
BSA (100x)	0.1 µL
Total	**10.1 µL**

3.1.2 Preparation of tetO-hM3Dq-mCherry Plasmid

3.1.2.1 Invertion of mCherry- hM3Dq Sequence

Original construct of the plasmid (Figure 2.3) has the inverted version of hM3Dq-mCherry sequence. As a result, promoter can not drive the gene. mCherry-hM3Dq sequence needed to be inverted and placed like in Figure 3.3 to be able to express the receptor.
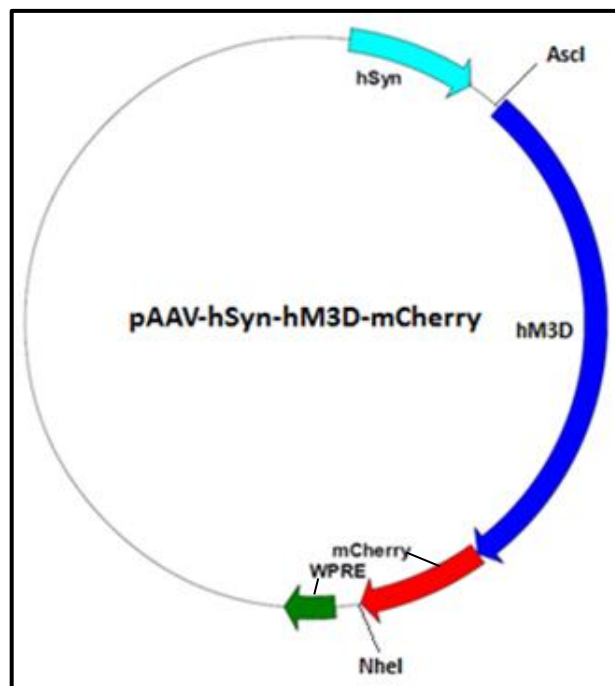
Figure 3. 3 Schematic construct of pAAV-hSyn-hM3D-mCherry.

PCR was conducted to amplify mCherry-hM3Dq sequence. 0.8% agarose gel was prepared and samples were run at 80 V for 60 minutes. The gel was screened and its picture was taken with gel imaging system. Figure 3.4 shows the band for mCherry-hM3Dq. After gel electrophoresis, correct band was cut out with the help of a surgical blade and purified.
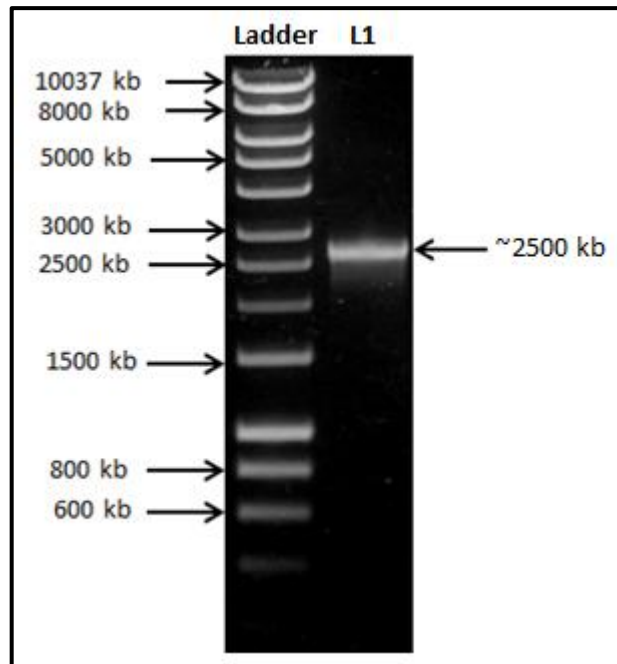
Figure 3. 4 PCR result for amplification of mCherry-hM3Dq sequence from pAAV-hSyn-double floxed-hM3D-mCheery. L1: PCR product.

Purified PCR product (insert) and pAAV-hSyn-double floxed-hM3D-mCherry plasmid (backbone) are doubled-digested with the restriction enzymes AscI and NheI. Digestion reaction was prepared with a composition shown in the Table 3.2 and incubated at 37°C for 2 hours.

Table 3. 2 Components of the digestion reaction to obtain insert and backbone.

	Insert	Backbone
PCR product	10 μL	X
hSyn-mCherry-hM3Dq plasmid	X	10 μL
ddH₂O	10.7 μL	10.7 μL
NheI	3 μL	3 μL
AscI	3 μL	3 μL
NEBuffer 4	3 μL	3 μL
BSA (100x)	0.3 μL	0.3 μL
Total	30 μL	30 μL

0.8% agarose gel was prepared and bacbone digestion products were loaded. Samples and ladder were run at 80 V for 60 minutes. The gel was screened and its picture was

taken with gel imaging system (Figure 3.5). hSyn-backbone band was cut with the help of a surgical blade and purified. Digestion products of insert were purified with PCR Product Purification Kit.

Concentrations of samples were measured with Nanodrop. Insert (hM3Dq-mCherry sequence) and backbone (pAAV-hSyn-backbone) were ligated with the ratios of 1:3, 1:5, Max and negative control (Table 3.3). Negative control was only consisted of backbone and ligated to itself. Quick Ligation Kit was used for the reaction. After all components were added, ligation reaction was carried out at room temperature for 30 minutes.

6 colonies were picked (max ligation) and incubated LB Broth overnight. Plasmid DNA was purified and isolated. Thus, pAAV-hSyn-hM3Dq-mCherry construct was acquired.
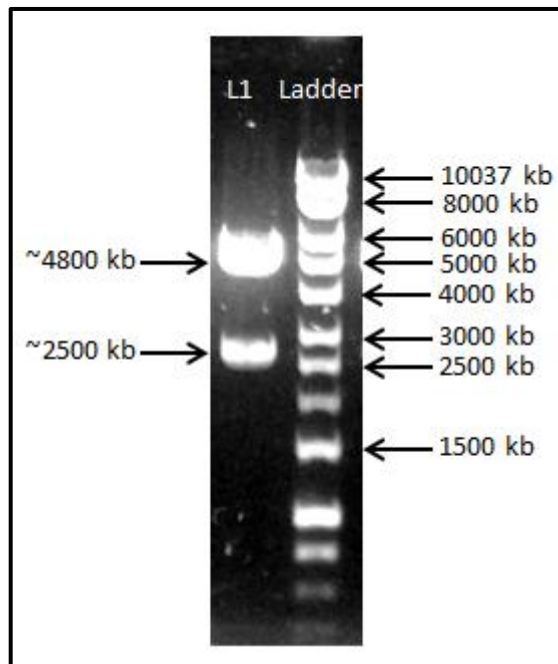
Figure 3. 5 Gel picture of pAAV-hSyn-double floxed-hM3D-mCherry after double digestion reaction. pAAV-hSyn-backbone: around 4800 kb; hM3Dq-mCherry sequence: around 2500 kb.

Table 3. 3 Components of ligation reactions of pAAV-hSyn-backbone and hM3Dq-mCherry sequence.

Ratio	1:3	1:5	Max	Negative Control
Backbone	2 μL	2 μL	2 μL	2 μL
PCR product/Insert	1 μL	1.5 μL	8 μL	X
Buffer	10 μL	10 μL	10 μL	10 μL
ddH$_2$O	7 μL	6.5 μL	X	8 μL
Quick T4 DNA Ligase	1 μL	1 μL	1 μL	1 μL

3.1.2.2 tetO-hM3Dq-mCherry Construct

Human Synapsin Promoter (hSyn) needed to be replaced by tetO promoter to complete Tet-Off system. pAAV-hSyn-hM3Dq-mCherry plasmids were doubled-digested with the restriction enzymes MluI and SalI. Digest reaction was prepared with components shown in the Table 3.4 and incubated at 37°C for 2 hours.

**Table 3. 4** Components of the digest reaction to obtain hM3Dq-mCherry backbone.

pAAV-hSyn-hM3Dq-mCherry plasmid	2 μL
ddH$_2$O	5 μL
MluI	1 μL
SalI	1 μL
NEBuffer 3	1 μL
BSA (100x)	0.1 μL
Total	10.1 μL

0.8% agarose gel was prepared and bacbone digestion products were loaded. Samples and ladder were run at 80 V for 60 minutes. The gel was screened and its picture was taken with gel imaging system (Figure 3.6). hM3Dq-mCherry-backbone band was cut with the help of a surgical blade and purified. Digestion product of insert were purified with PCR Product Purification Kit.
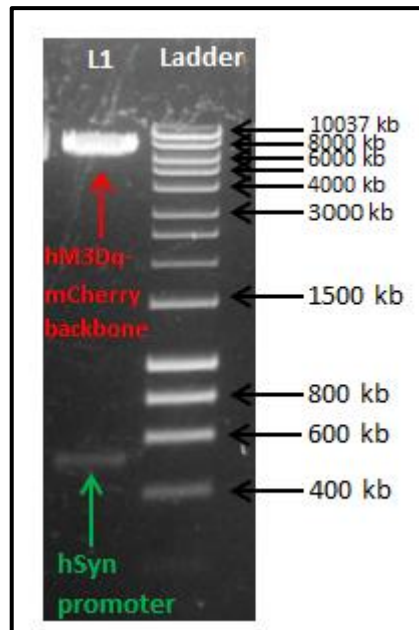
Figure 3. 6 Double digestion of pAAV-hSyn-hM3Dq-mCherry plasmid with MluI and SalI restriction enzymes. L1: digest products. hM3Dq-mCherry-backbone: ~6800 kb; hSyn promoter: ~500 kb.

Concentrations of tetO promoter and hM3Dq-mCherry-backbone were measured with Nanodrop. Insert (tetO promoter) and backbone (hM3Dq-mCherry) were ligated with the ratios of 1:3, 1:5, 1:7, Max and negative control (Table 3.5). Quick Ligation Kit was used for the reaction. After all components were added, ligation reaction was carried out at room temperature for 30 minutes.

Table 3. 5 Components of ligation reactions for tetO-hM3Dq-mCherry construct.

Ratio	1:3	1:5	1:7	Max	Negative Control
Backbone	3 µL	3 µL	3 µL	3 µL	3 µL
tetO promoter	0.5 µL	1 µL	1.5 µL	7 µL	X
Buffer	10 µL	10 µL	10 µL	10 µL	10 µL
ddH$_2$O	6.5 µL	6 µL	5.5 µL	X	7 µL
Quick T4 DNA Ligase	1 µL	1 µL	1 µL	1 µL	1 µL

12 colonies were picked (max ligation) and incubated LB Broth overnight. Plasmid DNA was purified and isolated. Thus, tetO-hM3Dq-mCherry construct was acquired. A digestion reaction was carried out to check if the ligation was successful. tetO-hM3Dq-mCherry plasmids were doubled-digested with the restriction enzymes MluI and NheI.

Digestion reaction was prepared with components shown in the Table 3.6 and incubated at 37°C for 2 hours.

Table 3. 6 Components of the double digestion reaction to check tetO-hM3Dq-mCherry construct.

tetO-hM3Dq-mCherry	2 µL
ddH₂O	6 µL
MluI	0.5 µL
NheI	0.5 µL
NEBuffer 2	1 µL
BSA (100x)	0.1 µL
Total	**10.1 µL**

0.8% agarose gel was prepared and digestion products were loaded to gel. Samples and ladder were run at 80 V for 40 minutes. The gel was screened and its picture was taken with gel imaging system (Figure 3.7). After gel electrophoresis, positive samples were sent sequencing. Sequencing results verified the construct for tetO-hM3Dq-mCherry plasmid.
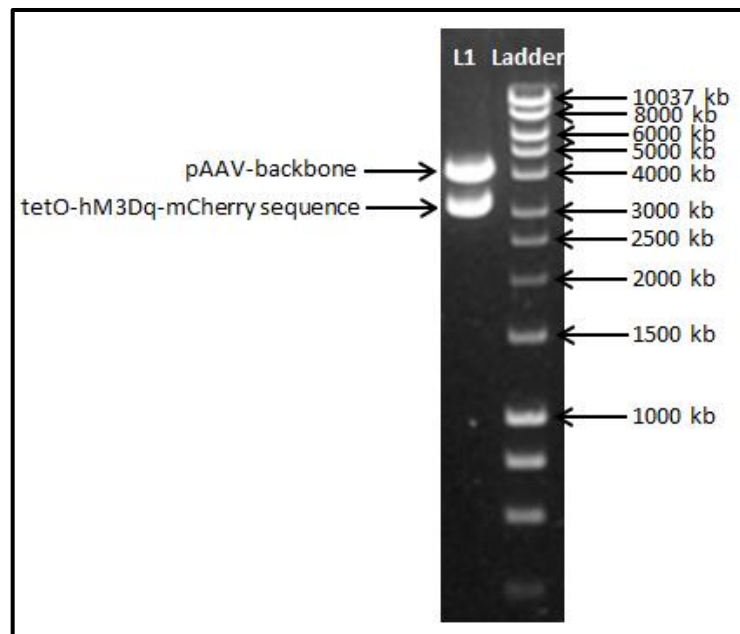
Figure 3. 7 Double digestion of tetO-hM3Dq-mCherry with MluI and NheI restriction enzymes. L1: double digestion products. pAAV-backbone: ~4300 kb; tetO-hM3Dq-mCherry sequence: ~3000 kb.

3.1.3 Preparation of tetO-hM4Di-mCherry Plasmid

3.1.3.1 Invertion of mCherry- hM4Di Sequence

Original construct of the plasmid (Figure 2.4) has the inverted version of hM4Di-mCherry sequence. As a result, promoter can not drive the gene. mCherry-hM4Di sequence needed to be inverted and placed like in Figure 3.8 to be able to express the receptor.
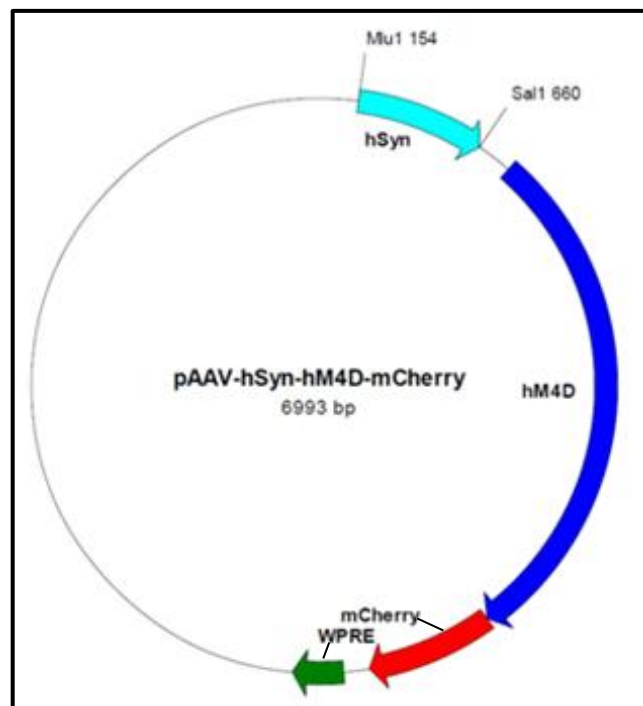
Figure 3. 8 Schematic construct of pAAV-hSyn-mCherry-hM4Di plasmid.

PCR was conducted to amplify mCherry-hM4Di sequence. 0.8% agarose gel was prepared and samples were run at 80 V for 40 minutes. The gel was screened and its picture was taken with gel imaging system. Figure 3.9 shows that the band for mCherry-hM4Di. After gel electrophoresis, the band at L6 was cut with the help of a surgical blade and purified. PCR components and conditions for L1 to L5 is not given due to negative result. *Pfu* enzyme was used for PCR from L1 to L4 and Green Mix was used at L5 for the amplification of mCherry-hM3Dq sequence. L6 is positive result and Green Mix was used at L6 for the amplification of mCherry-hM4Dq sequence.
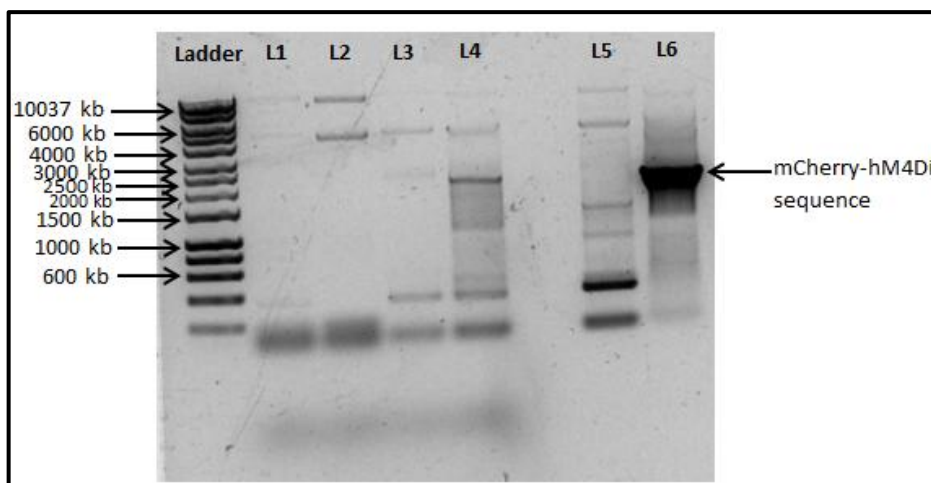
Figure 3. 9 PCR products for amplification of mCherry-hM3Dq and mCherry-hM4Di sequence. L1 to L4: negative PCR results with *Pfu* enzyme. L5: negative PCR result with Green Mix. L6: Positive PCR result for amplification of mCherry-hM4Di sequence.

Purified PCR product for mCherry-hM4Di sequence was doubled-digested with the restriction enzymes NheI and AscI. Digestion reaction was prepared with components shown in the Table 3.7 and incubated at 37°C for 2 hours.

Table 3. 7 Components of the digestion reaction to obtain hM4Di-mCherry insert and pAAV-hSyn-backbone.

	Insert	Backbone
PCR Product (mCherry-hM4Di)	10 μL	X
pAAV-hSyn-DIO-hM4D-mCherry Plasmid	X	10 μL
ddH₂O	10.7 μL	10.7 μL
NheI	3 μL	3 μL
AscI	3 μL	3 μL
NEBuffer 4	3 μL	3 μL
BSA (100x)	0.3 μL	0.3 μL
Total	**30 μL**	**30 μL**

Concentrations of insert and backbone were measured with Nanodrop. Insert (hM4Di-mCherry sequence) and backbone (pAAV-hSyn construct) were ligated at max ratio and one negative control was prepared (Table 3.8). After all components were added, ligation reaction was carried out at room temperature for 30 minutes.

Table 3. 8 Components of ligation reactions of pAAV-hSyn-backbone and hM4Di-mCherry sequence.

Ratio	Max	Negative Control
Backbone	2 μL	2 μL
Digestion Product	8 μL	X
Buffer	10 μL	10 μL
ddH$_2$O	X	8 μL
Quick T4 DNA Ligase	1 μL	1 μL

6 colonies were picked (max ligation) and incubated LB Broth overnight. Plasmid DNA was purified and isolated. Thus, pAAV-hSyn-hM4Di-mCherry construct was acquired.

3.1.3.2 tetO-hM4Di-mCherry Construct

Human Synapsin promoter (hSyn) needed to be replaced by tetO promoter to complete Tet-Off system. hSyn-hM4Di-mCherry plasmid (Figure 3.8) are doubled-digested with the restriction enzymes MluI and SalI. Digestion reaction was prepared with a components shown in the Table 3.9 and incubated at 37°C for 2 hours.

Table 3. 9 Components of the digestion reaction of hM4Di-mCherry with MluI and/or SalI .

	MluI-Only	SalI-Only	Double Digestion (MluI+SalI)
pAAV- hSyn-hM4Di-mCherry plasmid	2 μL	2 μL	2 μL
ddH$_2$O	6 μL	6 μL	5 μL
MluI	1 μL	X	1 μL
SalI	X	1 μL	1 μL
NEBuffer 3	1 μL	1 μL	1 μL
BSA (100x)	X	0.1 μL	0.1 μL
Total	10 μL	10.1 μL	10.1 μL

0.8% agarose gel was prepared and digestion products were loaded to gel. Samples and ladder were run at 85 V for 35 minutes. The gel was screened and its picture was

taken with gel imaging system (Figure 3.10). hM4Di-mCherry backbone was cut with the help of a surgical blade and purified.
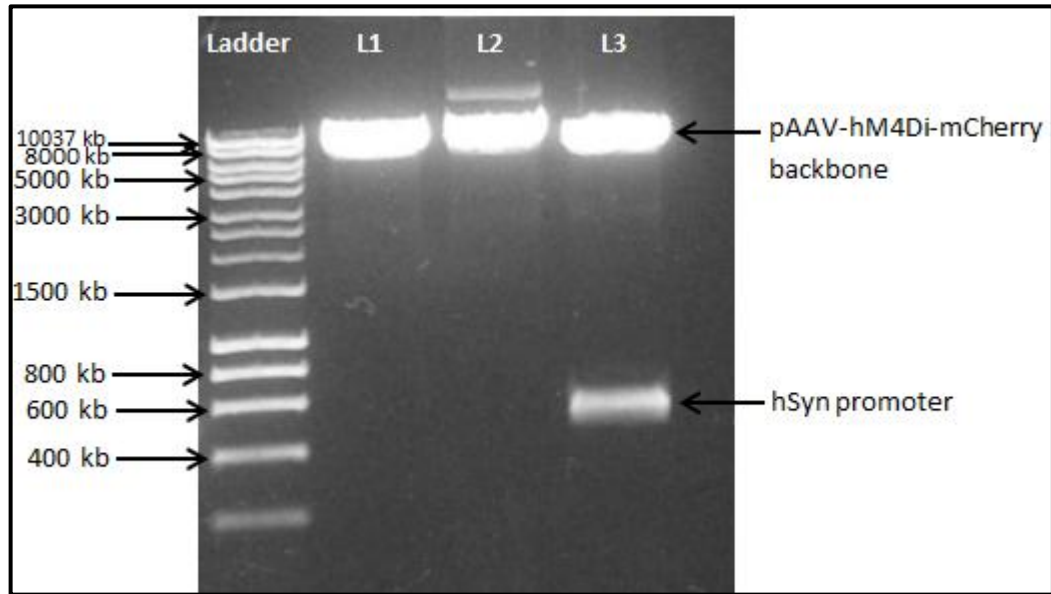
Figure 3. 10 Digestion results of pAAV-hSyn-hM4Di-mCherry plasmid with MluI and/or SalI. L1: MluI-only digestion; L2: SalI-only digestion; L3: double digestion with MluI and SalI. pAAV-hM4Di-mCherry backbone: ~6500 kb; hSyn promoter: ~500 kb.

Concentrations of the tetO promoter and hM4Di-backbone were measured with Nanodrop. Insert (tetO promoter) and backbone (pAAV-hM4Di-mCherry) were ligated at max ratio and one negative control was prepared (Table 3.10). After all components were added, ligation reaction was carried out at room temperature for 30 minutes.

Table 3. 10 Components of ligation reactions for tetO-hM4Di-mCherry construct.

Ratio	Max	Negative Control
hM4Di-mCherry backbone	2 μL	2 μL
tetO promoter	8 μL	X
Buffer	10 μL	10 μL
ddH₂O	X	8 μL
Quick T4 DNA Ligase	1 μL	1 μL

12 colonies were picked from max ligation and incubated in LB Broth overnight. Plasmid DNA was purified and isolated. A digestion reaction was carried out to check if the ligation was successful. tetO-hM4Di-mCherry plasmids were doubled-digested with

the restriction enzymes MluI and SalI. Digestion reaction was prepared with components shown in the Table 3.11 and incubated at 37°C for 2 hours.

Table 3. 11 Components of the digestion reaction to check tetO-hM4Di-mCherry construct.

tetO-hM4Di-mCherry plasmid	2 µL
ddH$_2$O	6 µL
MluI	0.5 µL
SalI	0.5 µL
NEBuffer 3	1 µL
BSA (100x)	0.1 µL
Total	**10.1 µL**

0.8% agarose gel was prepared and digestion products were loaded to gel. Samples and ladder were run at 85 V for 40 minutes. The gel was screened and its picture was taken with gel imaging system (Figure 3.11). After gel electrophoresis, positive samples were sent sequencing. Sequencing results verified the construct for tetO-hM4Di-mCherry plasmid.
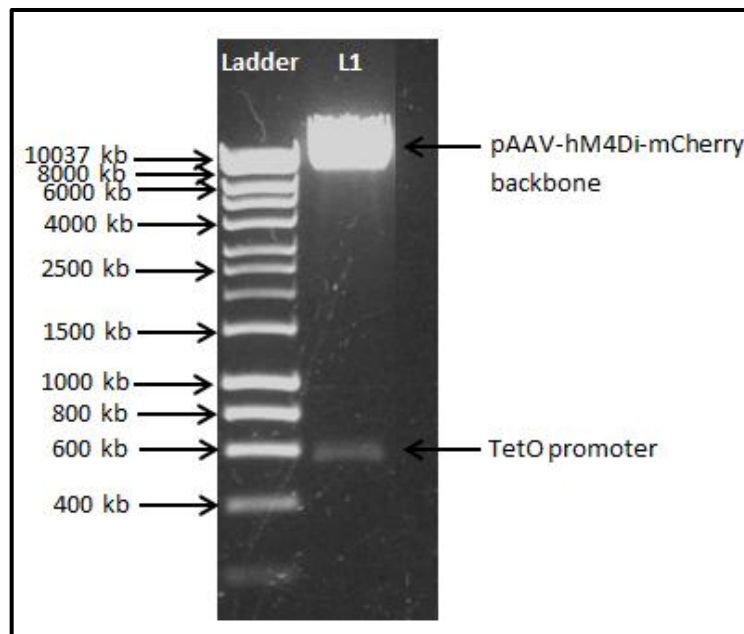
Figure 3. 11 Double digestion of tetO-hM4Di-mCherry with MluI and SalI restriction enzymes. L1: double digest product. pAAV-hM4Di-mCherry backbone: ~6500 kb; tetO promoter: ~500 kb.

3.1.4 SDS-PAGE Analysis of cfos-tTA in AAV, tetO-hM3dq in AAV and tetO-hM4Di in AAV

Three plasmids (cfos-tTA, tetO-hM3dq and tetO-hM4Di) were packaged into AAV1/2 vector. SDS-PAGE was perfomed to confirm whether three AAV vectors that have been packaged are pure and have only three capsid proteins. As Figure 3.12 shows, all of them has three bands from the three capsid proteins at the molecular weight of 90 kDa, 60 kDa and 50 kDa.
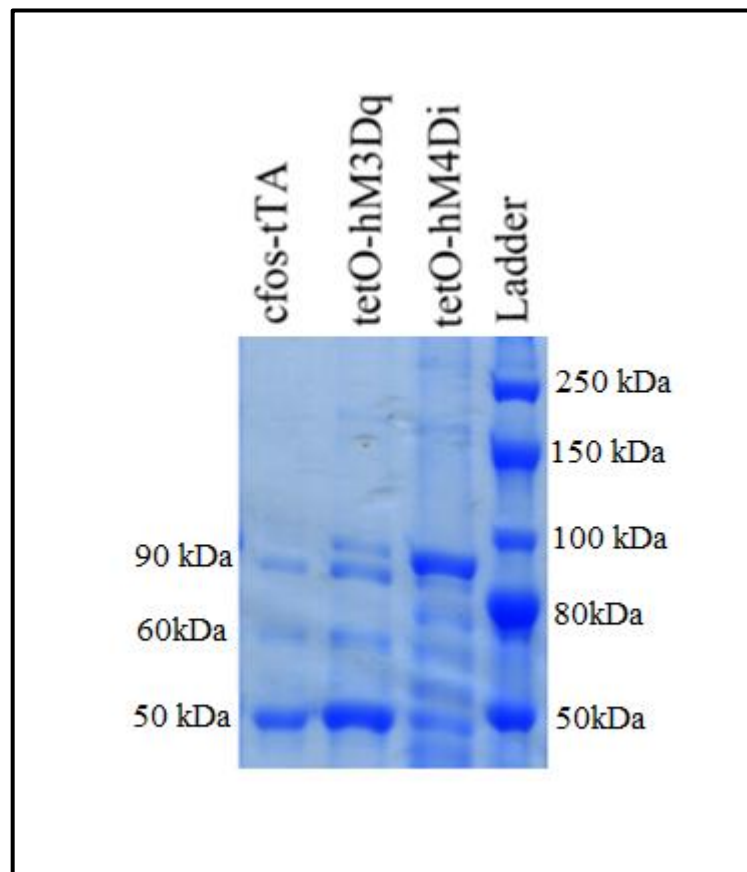
Figure 3. 12 Gel picture of SDS-PAGE for cfos-tTA in AAV, tetO-hM3dq in AAV and tetO-hM4Di in AAV.

3.2 Immunohistochemistry Results

3.2.1 Immunohistochemistry with cFos Monoclonal Antibody

In study that carried out by Basheer et al. [60], IHC results showed that cingulate cortex region of rats are highly active during wake state but silent while they are asleep (Figure 3.13).
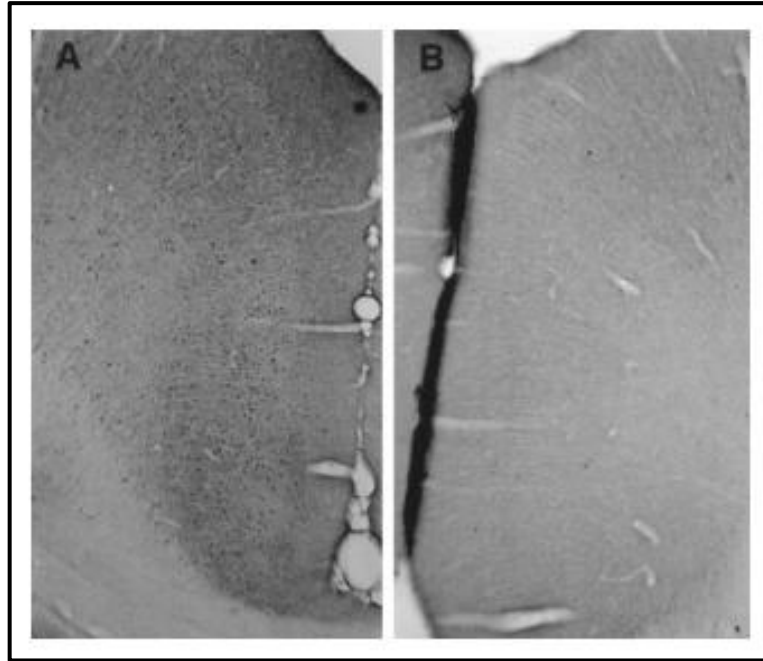
Figure 3. 13 Immunohistochemistry detection of cFos in rats. (**A**) IHC results after sleep deprivation for 12 hours in cingulate cortex. (**B**) IHC results after recovery sleep for 1 hour in cingulate cortex [60].

The results of immunohistochemical investigations for cFos are given in Figure 3.14. VLPO region is significantly active during recovery sleep. However, a few cfos-labelled cells can be detected while the animal was awake (SD, VLPO) when it is compared to the results with recovery sleep (SD+RS, VLPO). In other words, neuronal activity in VLPO was increased during sleep. Therefore, we can see many c-fos labeled cells in the left hand side bottom image. The IHC results compared with the results from Basheer et al. [60]. As expected, cingulate cortex has plenty of cFos-labelled cells during sleep deprivation (SD, Cing) but none during recovery sleep (SD+RS, Cing) [60]. Because sleep-active neurons are active during recovery sleep and as a result cfos is expressed.
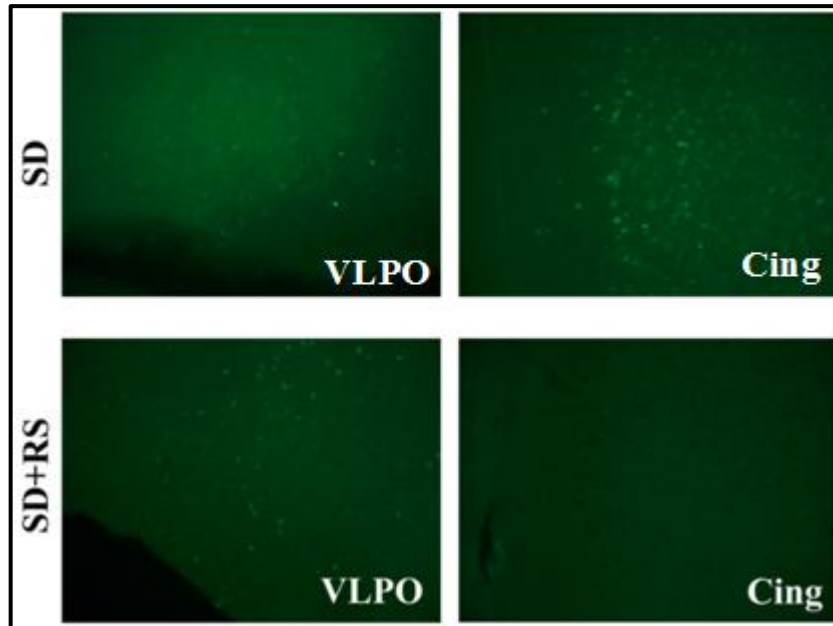
Figure 3. 14 Immunohistochemistry detection of cFos in mouse. Left hand sight images show VLPO region which significantly active during sleep (bottom image) but not wake state). Right hand sight images show cingulate cortex area during sleep (bottom image) and wake state (top image). SD, sleep deprivation; SD+RS, sleep deprivation and recovery sleep; Cing, cingulate cortex. Magnification, X10.

3.2.2 Immunohistochemistry with Anti-mCherry Monoclonal Antibody

Lu et al. [61] showed VLPO region in rats has high neuronal activity during sleep and as a result, cFos immunoreactivity of the neurons in VLPO were increased drastically in spontaneous sleep (Figure 3.15).

The results of our first immunohistochemical investigations for anti-mCherry are given in Figure 3.16. Far left hand side image is the result of anti-mCherry antibody staining. It shows that two viruses can infect one cell at the same time when they co-injected. Expression of tetO-hM3Dq can not be activated without tTA protein binding to tetO promoter and to express tTA, cfos promoter must be activated (Figure 3.17). Immunohistochemistry results was merged with the DAPI (4',6-diamidino-2-phenylindole) staining image in the middle to verify cfos IHC results.
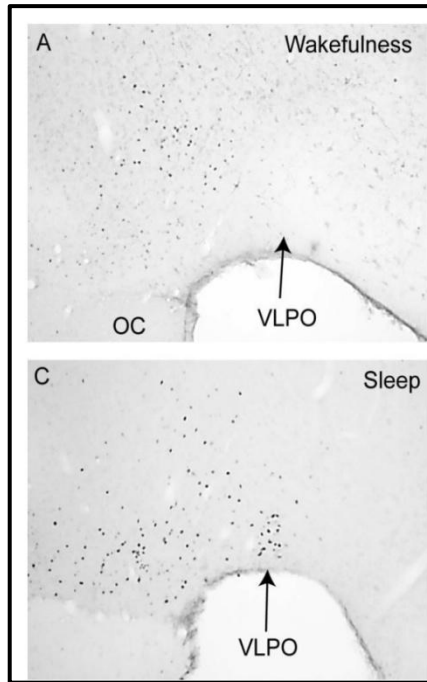
Figure 3. 15 Fos expressions in VLPO during wake and sleep state. (**A**) Fos expression in VLPO during wakefulness, and (**C**) Fos expression in VLPO during sleep. Adapted from Lu et al. [61].
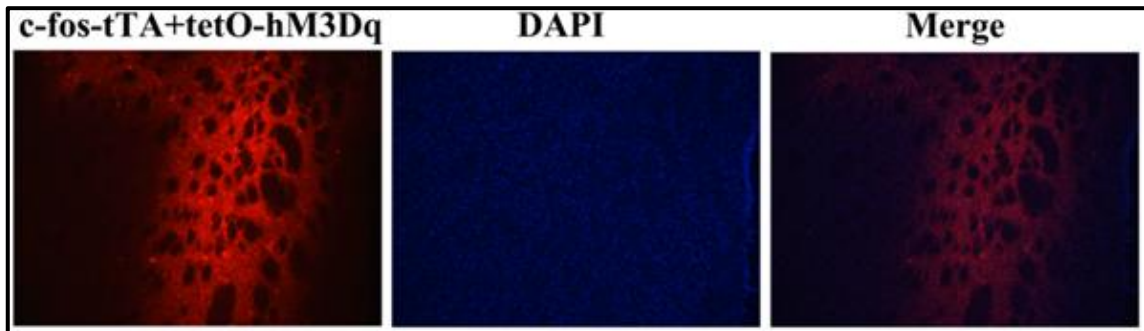
Figure 3. 16 Immunohistochemistry investigation of co-injection of c-fos-tTA in AAV and tetO-hM3Dq in AAV. Co-injections were made into caudate putamen region. Two images were merged using Photoshop (Adobe). Magnification, X20.
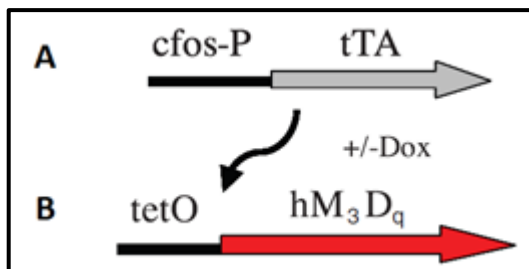
Figure 3. 17 Activation of tetO-hM3Dq transgene (**B**) under the control of first transgene (**A**). Adapted from Garner et al. [52].

The results of the second immunohistochemical investigations for anti-mCherry are given in Figure 3.18. While the virus expression can be barely seen on ON DOX mice, on OFF DOX mice (both OFF DOX 12H and OFF DOX 3DAYS) spread of virus can be seen clearly. Furthermore, it can be clearly seen that the virus expression was increased simultaneously with off Dox time.

Because injections for tetO-hM4Di-mCherry viruses were not targetted well, no IHC result for tetO-hM4Di virus-injected mice were obtained.
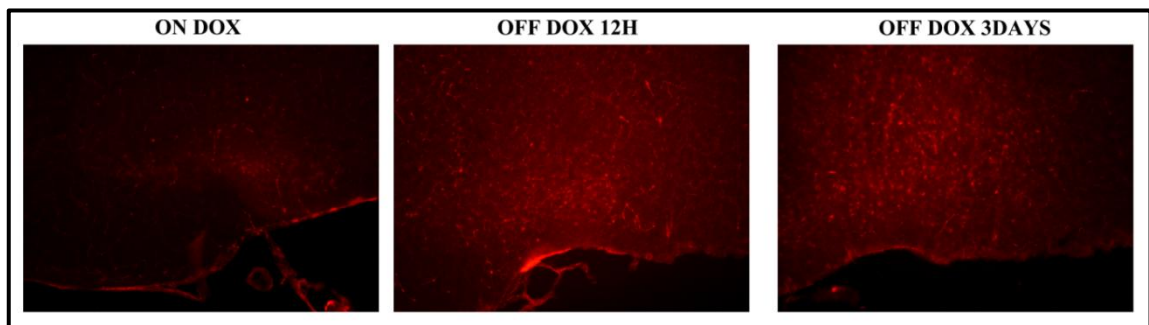
Figure 3. 18 Anti-mCherry IHC detection of tetO-hM3Dq-mCherry virus expression in VLPO which is regulated by Dox. Magnification, X10.

3.3 EEG/EMG Recording Analysis

3.3.1 Sleep Scoring and Power Spectral Analysis

EEG and EMG data in neurologer was downloaded and converted to text file (Figure 3.19). Data file was imported into Spike 7 software. Prior to scoring, all EcoG and EMG channels were filtered out for the frequencies below 0.5 Hz to remove low frequency noise. An algorithm with *if-then-else* logic used that is defined by Costa-Miserachs et al. [58] to clasify signals as Wake, NREM or REM. The algorithm is determined the sleep score according to theta:delta ratio (Table 3.12). Delta refers to frequencies 0 to 4 Hz while theta refers to 6 to 10 Hz. If the algorithm can not score the signals, it marks it as "doubt" and subsequently user can correct it manually [58].

One sample was chosen for each of On-Dox and Off-Dox recordings to obtain sleep scores and perform power spectral analysis. Figure 3.20 and Figure 3.21 are the sleep scores after CNO injection of these recordings. When Figure 3.20 and Figure 3.21 were compared, there is a significant increase in NREM sleep period. Nearly 1500 seconds of increase in NREM sleep was observed (Figure 3.21). Figure 3.22 and Figure 3.23 are the

power spectral graphs to see the effects of CNO injection upon electrical activity of the brain. Control mouse shows similar results before and after CNO injection in Figure 3.22, but still, there is shift from 8 Hz theta frequency to 10 Hz theta frequency depending on CNO stimulation. However on SD+Off-Dox animal, the power shift can be seen from 8-10 Hz (alpha) to 1-4 Hz (delta) in power spectrum graph (Figure 3.23). The shift from alpha to delta between before and after CNO injection results shows that after CNO injection, Off-Dox mouse often goes into SWS.
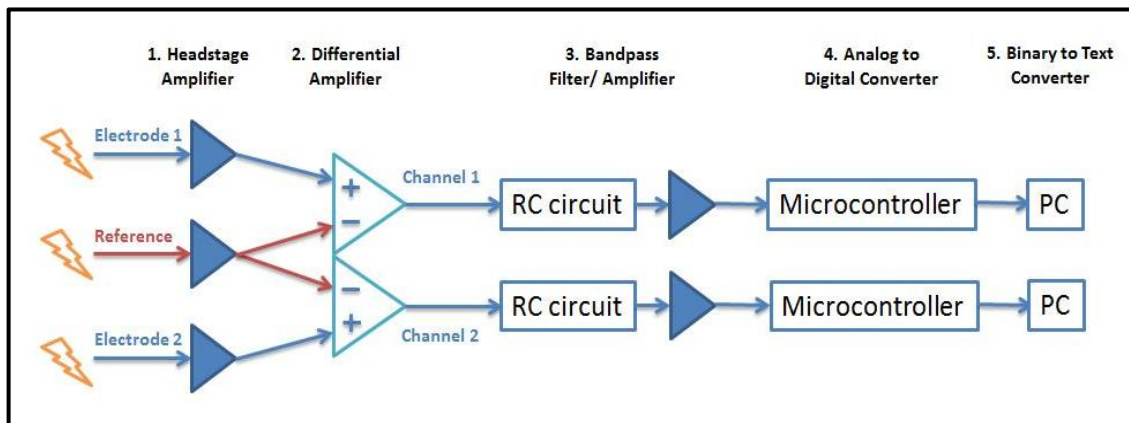
Figure 3. 19 A simplified schematic of key elements in the Neurologger 2. EcoG and EMG signals are picked up as electrical potential from EEG electrodes and they are amplified when they entered the headstage (Step 1). The reference signals are removed from other two electrode's signal and amplified (Step 2). The two EEG and two EMG channels (except reference channels) are bandpass filtered by Resistor-Capacitor Circuit (Step 3) and amplified. In microcontroller filtered signals are converted from analog to digital (200 Hz) signal (Step 4). When neurologger is connected with PC via USB connection, the digital signals that recorded in binary are converted into text format (Step 5). This process is repeated for all three EEG and three EMG channels [57].

Table 3. 12 Criteria for sleep scoring.

Stage	Criteria
Wake	High EMG and intermediate theta: delta ratio
NREM Sleep	EMG lower than Wake and high delta
REM Sleep	Low EMG and high theta:delta ratio
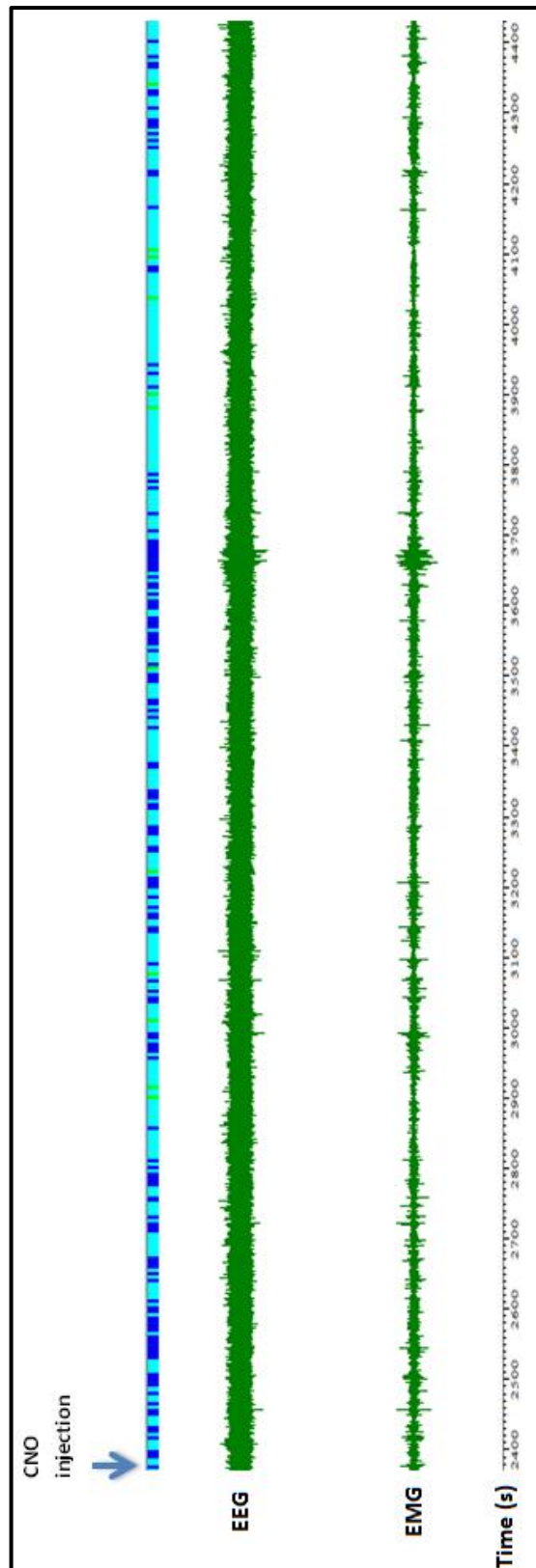
Figure 3. 20 Filtered sleep score for On Dox mouse after CNO injection. The color scale on top indicates pattern of sleep-wake. Dark blue color refers wakefulness, light blue refers REM sleep while green refers NREM sleep.
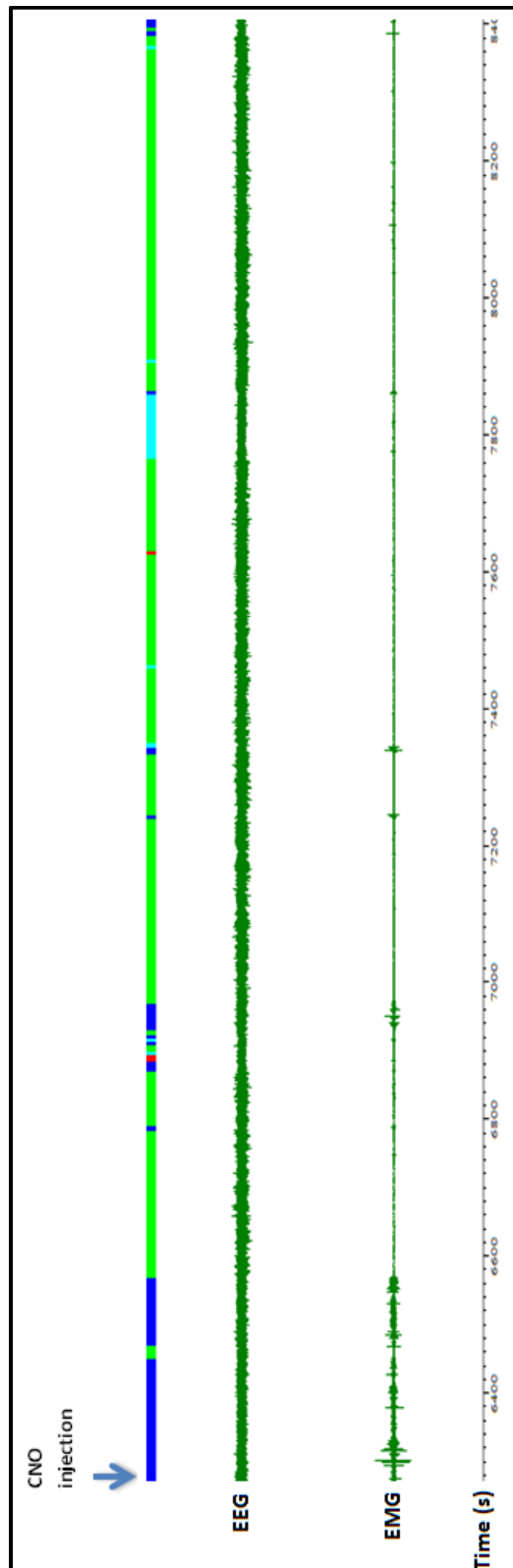
Figure 3. 21 Filtered sleep score after CNO injection in sleep deprived+off Dox(12h) mouse. The color scale on top indicates sleep-wake state. Dark blue color refers wakefulness, red refers doubt, and light blue refers REM sleep while green refers NREM sleep.
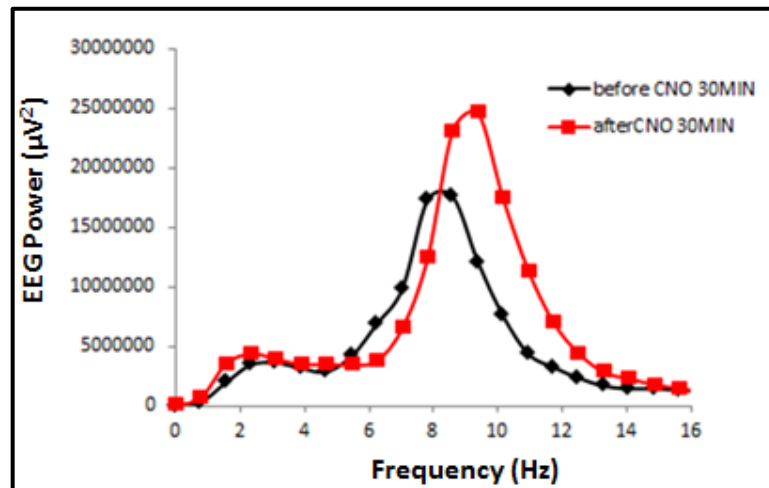
Figure 3. 22 Power spectral analysis of EEG recordings in On Dox mouse. The x-axis in the power spectrum represents the frequency band that was sampled, and the y-axis represents the power in that frequency band.
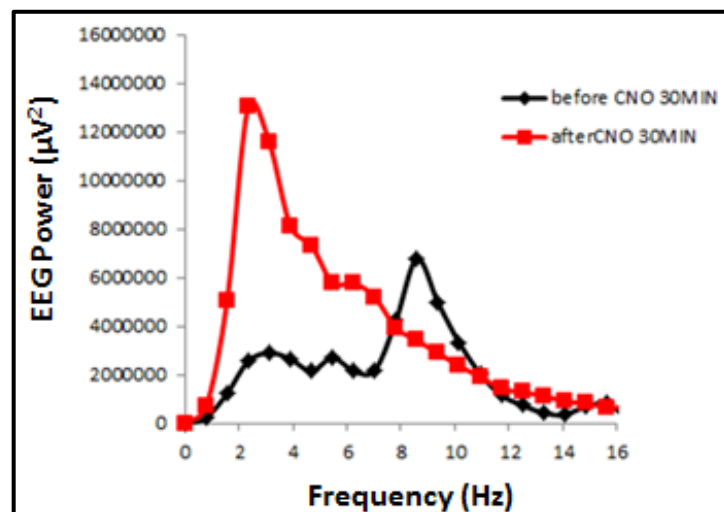
Figure 3. 23 Power spectral analysis of EEG recordings in SD+Off Dox mouse. The x-axis in the power spectrum represents the frequency band that was sampled, and the y-axis represents the power in that frequency band.

3.3.2 Morlet Wavelet Analysis

The Morlet Wavelet Transform is a kind of Continuous Wavelet Transform. It helps to analyze the change in frequency response with responce to time accurately. The most widely used tool for time-frequency analysis is Fourier Transform. However, it can not catch the change in frequency response with respect to time. According to Uncertainty Principle in quantum mechanics, it is impossible to differentiate variables precisely simultaniously. Which means, the more a variable is determined precisely, the less

precisely the other variable can be known. Wavelet is the best solution this problem. With wavelet transform, short time window, high frequency and long time window and low frequency can be processed together at the same time [62].

Since the EEG signal are not stationary, Morlet Wavelet can be used to process these signals. In Figure 3.24, the EEG data for control mouse is used and high amplitude band is between 5-9 Hz. Which means, most of the time animal is in drowsiness or awake.
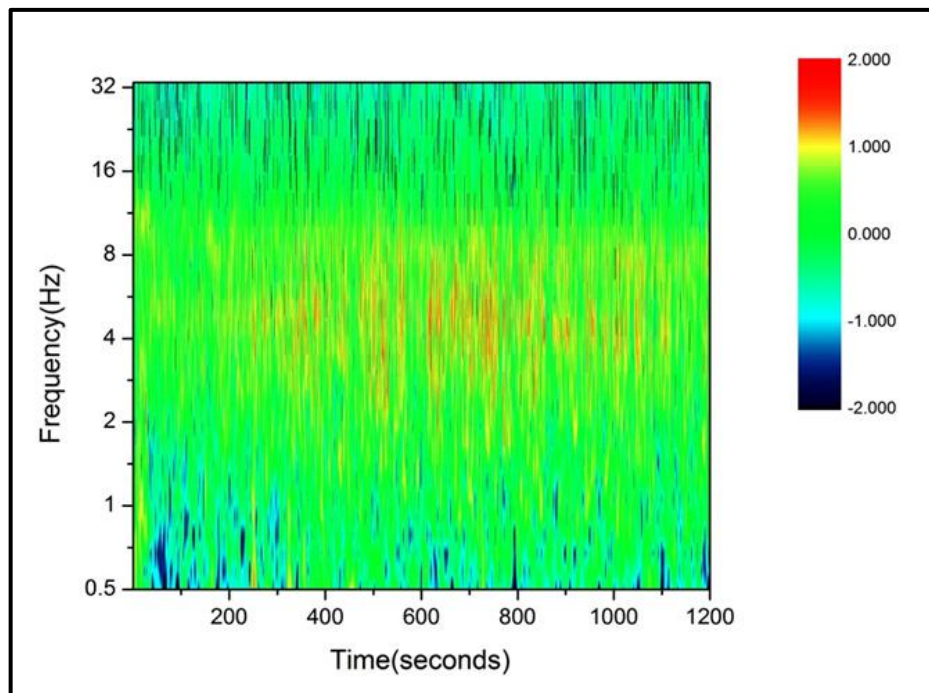
Figure 3. 24 EEG signals that investigated by Morlet Wavelet for On-Dox (Control) mouse after CNO injection.

In Figure 3.25, the EEG data for SD+Off-Dox(12h) mouse is used and high amplitude band is between 2-4 Hz. Which means, most of the time animal is in NREM sleep or deep sleep (delta).
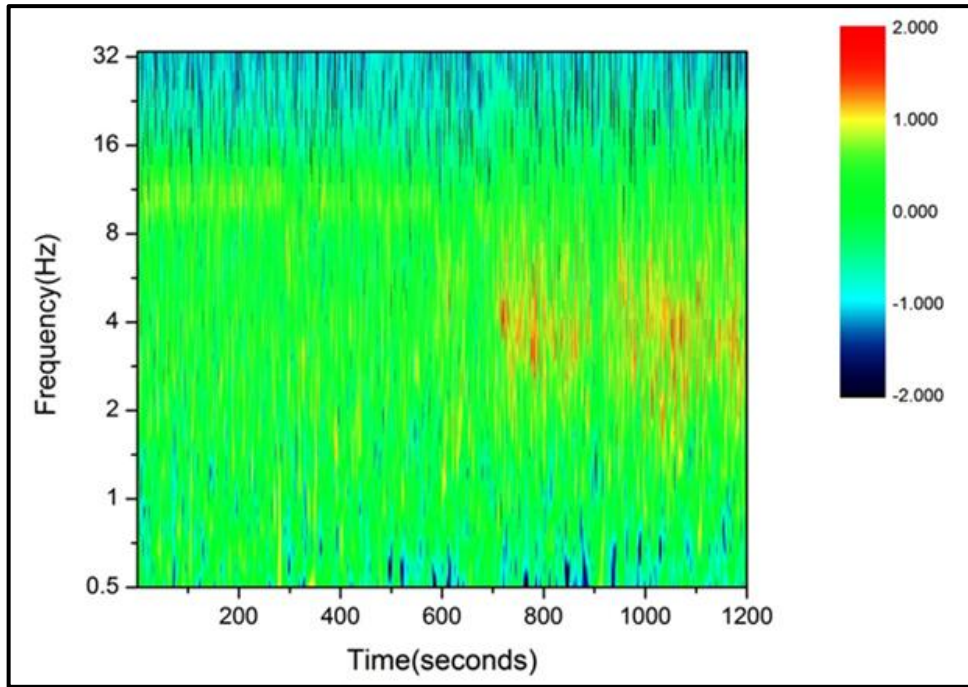
Figure 3. 25 EEG signals that investigated by Morlet Wavelet for SD+Off-Dox(12h) mouse after CNO injection.

In Figure 3.26, the result of direct activation of anterior hypothalamic nuclei by CNO injection after SD can be seen. In SD+OFF-DOX-12h mice, while percentage was decreased drastically, percentage of NREM was increased simultaniously (Figure 3.26).
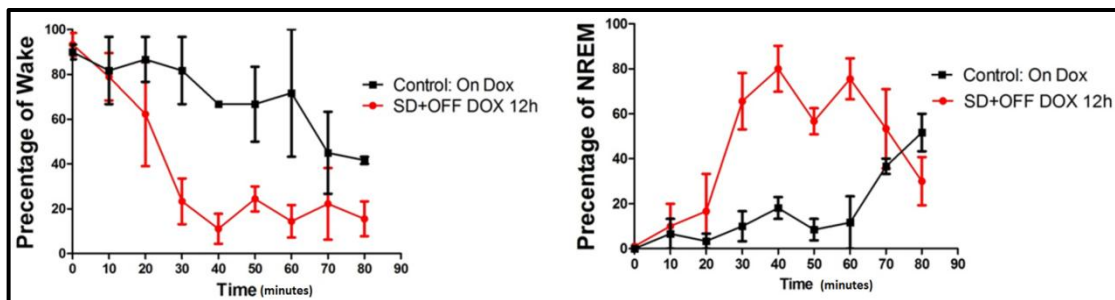
Figure 3. 26 Percentage of Wake and NREM sleep by time in control (n=5) and SD+OFF-DOX-12h (n=5) after CNO injection.

3.4 Animal Behavior Test Analysis

Experiment results based on total travel distance were observed as seen at Figure 4.27 (a) for both group. There is a significant reduction in travel distance of animal at CNO-injected group. While travel distance of control mice was decreasing by the time due to acclimatization, travel distance of CNO-injected mice is relatively stable and less than control group (Figure 3.27 b).
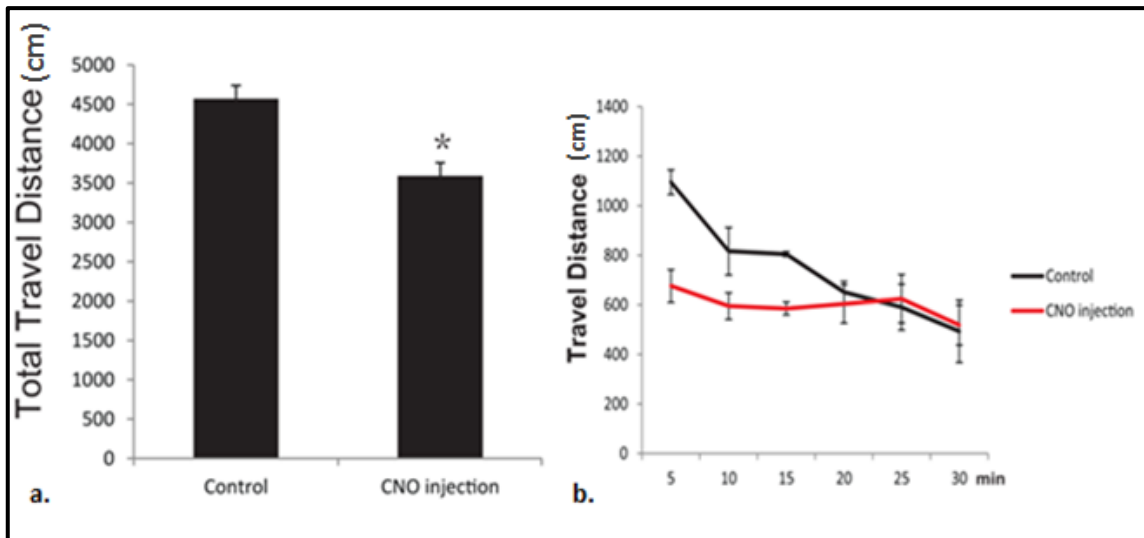
Figure 3. 27 Graphs of total travel distance of conrol and CNO injection. (**a**) Comprasion of control (n=4) and CNO-injected (n=4) group based on total travel distance (*p* < 0.005, paired *t* test, tails: 2). (**b**) The distance that animal travelled for every five second for control and CNO-injected group.

On-Dox mice showed significantly high total travel distance due to Dox administration all the time. Doxycyline prevented expression of hM3Dq on On Dox mice. Therefore, CNO injection didn't affect them. However, hM3Dq were able to expressed when Dox administration stopped for Off-Dox-12h and Off-Dox-4-Weeks mice. Consequently, total travel distance results were dropped. Because the viruses started to lose their effect on Off Dox 4 Weeks mice, average for Off-Dox-4-Weeks mice is higher than Off-Dox-12h mice (Figure 3.28).
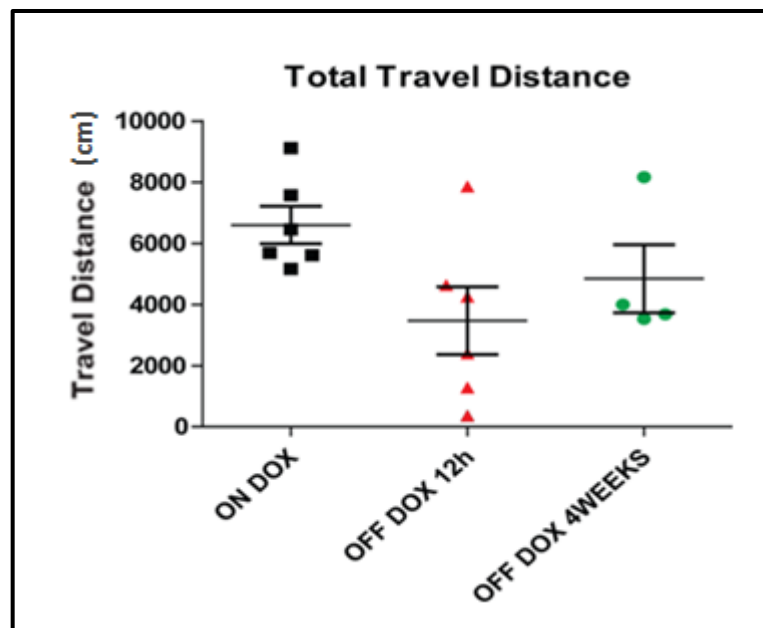
Figure 3. 28 Locomoter test activity regulated by Dox administration.

3.5 Discussion

There have been many previous studies investigating various aspects of sleep-wake regulation. Majority of the studies mainly focus on c-Fos expression levels of several sleep-wake related brain regions [63, 64] and activation or inhibition of sleep- or wake-active receptors [65, 66, 67]. These studies, as well as many others, have shown preoptic area (POA), lateral hypothalamic area (LHA), basal forebrain (BF) and basal ganglia (BG) have an important role on sleep/wake promotion which is hypothetically explained by flip-flop model [63, 64, 68, 69].

Recently there have been several studies that have investigated sleep-wake regulation with new approaches like DREADDs and knock-out animal studies [65, 66, 70]. Lazarus et al. [66] used two different $A_{2A}R$ knock-out mice (global and BG) and focal RNA interference to block adenosine A_{2A} receptors. They found that adenosine A_{2A} receptors in nucleus accumbens are responsible for promotion of wakefulness by caffeine [66]. Sasaki et al. [65] used DREADD system to activate and suppress orexin neurons in LHA. They concluded that activation orexin neurons were successfully manipulated by DREADD system. By the activation of orexin neurons, total amount of wakefulness increased and total amount of NREM and REM sleep decreased significantly [65]. Saito et al. [70] also applied DREADD system to control POA GABAergic neurons. They found stimulation of GABAergic neurons leads to increase in NREM sleep. Also, they found POA GABAergic neurons innervate with orexin neurons in *Gad67-Cre* mice by ChR2-eYFP (as an anterograde tracer) and optogenetic approach [70].

However, none of these studies have attempted to activate VLPO region selectively and reversibly to test flip-flop model. The objective of this thesis was to activate/inactivate VLPO selectively and reversibly by the microinjection of two transgene systems which was described by Garner et al. [52] and observe the effects of CNO administration via immunohistochemistry, animal behaviour tests and EEG recordings. Result of these analysis have shown that artificially-activated VLPO sleep-active neurons lead to sleep in genetically engineered mice and an increase in NREM sleep significantly.

CONCLUSION

4.1 Conclusion

Aim of this thesis has been to test flip-flop hypothesis in order to have a better understanding on sleep process. In this study, as the flip-flop hypothesis proposed, it has been speculated that when arousal neurons are inhibited and/or sleep-active neurons are activated in animals with two transgene system, animals should fall asleep. As expected, it has been observed that when sleep-active neurons in VLPO are activated artificially during wake state, sleep can be promoted in animals. Also, an increase in NREM sleep have been observed in genetically engineered mice. However, because of an experimental application problem, we could not get any data and result for hM4Di mice experiments. Therefore, we do not know if a wake state can be promoted in animals, when sleep-active neurons are inhibited during sleep state.

4.2 Future Perspective

These experiments gave a better comprehension of mechanisms of sleep promotion. However, the experiments with hM4Di mice should be repeated again to have a deeper understanding on sleep promotion. It is known that the targeted region VLPO contains a very large population of sleep-active neurons [71], however in the present study we did not have any knowledge of which cell types are infected. Future research should therefore concentrate on the investigation of identification of those cell types. Besides, more research is required on different brain regions like MnPN to develop better understanding on sleep-active neurons.

REFERENCES

[1]   Carskadon, M.A. and Dement, W.C., (2011). Principles and Practice of Sleep Medicine, 5th Edition, Editors: Kryger, M.H., Roth, T., and Dement, W.C., Saunders Elsevier, St. Louis.

[2]   Colten, H.R., Altevogt, B.M., (2006). Sleep disorders and sleep deprivation: an unmet public health problem, Editors: Institute of Medicine Committee on Sleep Medicine and Research, Institute of Medicine, National Academies Press, Washington, DC.

[3]   Savage, V. M. and West, G. B. (2007). "A quantitative, theoretical framework for understanding mammalian sleep", Proc Natl Acad Sci USA, 104(3): 1051-1056.

[4]   Selam Higher Clinic, Anatomical and physiological bases of consciousness and sleep wake cycle, http://www.selamhigherclinic.com/resources/neurology/presentation/Anato Anato and physiological bases of consciousness and sleep.ppt, 18th October 2013.

[5]   Merica, H. and Fortune, R.D., (2004). "State transitions between wake and sleep, and within the ultradian cycle, with focus on the link to neuronal activity", Sleep Medicine Reviews, 8: 473–485.

[6]   Hirshkowitz, M. (2004). "Normal human sleep: an overview", Med Clin North Am, 88(3): 551-565.

[7]   Schabus, M., Gruber, G., Parapatics, S., Sauter, C., Klösch, G., Anderer, P., Klimesch, W., Saletu, B. and Zeitlhofer, J. (2004). "Sleep spindles and their significance for declarative memory consolidation", Sleep, 27(8): 1479-1485.

[8]   Lu, W. and Göder, R. (2012). "Does abnormal non-rapid eye movement sleep impair declarative memory consolidation?: Disturbed thalamic functions in sleep and memory processing", Sleep Med Rev, 16(4): 389-394.

[9]   Wamsley, E.J., Tucker, M.A., Shinn, A.K., Ono, K.E., McKinley, S.K., Ely, A. V., Goff, D.C., Stickgold, R. and Manoach, D.S. (2012). "Reduced sleep spindles and spindle coherence in schizophrenia: mechanisms of impaired memory consolidation?", Biol Psychiatry, 71(2): 154-161.

[10]   Horne, J.A. (2000). "REM sleep - by default?", Neurosci Biobehav Rev, 24(8): 777-797.

[11]   Berry, R.B. (2012). Fundamentals of sleep medicine, Elsevier/Saunders, Philadelphia, PA.

[12]   Siegel, J.M. (2005). Principles and practice of pediatric sleep medicine, Editors: Sheldon, S.H., Ferber, R. and Kryger, M.H., Elsevier Saunders, Philadelphia.

[13]   Lee-Chiong, T.L., Sateia, M.J. and Carskadon, M.A. (2002). Sleep medicine, Hanley & Belfus, Philadelphia.

[14]   Kohyama, J. (2000). "REM sleep atonia: responsible brain regions, quantification, and clinical implication", Brain Dev, 22: S136-142.

[15]   McCarley, R.W. (2007). "Neurobiology of REM and NREM sleep", Sleep Med, 8(4): 302-330.

[16]   Lee-Chiong, T. L. (2006). Sleep : a comprehensive handbook, Wiley, Hoboken, N.J.

[17]   Takahara, M., Kanayama, S. and Hori, T. (2009). "Co-occurrence of Sawtooth Waves and Rapid Eye Movements during REM Sleep", International Journal of Bioelectromagnetism, 11(3): 144-148.

[18]   Chokroverty, S., Allen, R.P. and Walters, A.S. (2013). Sleep and movement disorders, 2nd Ed., Editors: Chokroverty, S., Allen, R.P. and Walters, A.S., Oxford University Press, Oxford.

[19]   Vetrivelan, R., Chang, C. and Lu, J. (2011). "Muscle tone regulation during REM sleep: neural circuitry and clinical significance", Arch Ital Biol, 149(4): 348-366.

[20]   Lim, A.S., Lozano, A.M., Moro, E., Hamani, C., Hutchison, W.D., Dostrovsky, J.O., Lang, A.E.,Wennberg, R.A. and Murray, B. J. (2007). "Characterization of REM-sleep associated ponto-geniculo-occipital waves in the human pons", Sleep, 30(7): 823-827.

[21]   Escudero, M. and Márquez-Ruiz, J. (2008). "Tonic inhibition and ponto-geniculo-occipital-related activities shape abducens motoneuron discharge during REM sleep.", J Physiol, 586(14): 3479-3491.

[22]   Redfern, P.H., Waterhouse, J.M. and Minors, D.S. (1991). "Circadian rhythms: principles and measurement", Pharmacol Ther, 49(3): 311-327.

[23]   Markov, D., Goldman, M. and Doghramji, K. (2012). "Normal Sleep and Circadian Rhythms: Neurobiological Mechanisms Underlying Sleep and Wakefulness", Sleep Med Clin, 7: 417–426.

[24]   Edelstein, K. and Amir, S. (1999). "The role of the intergeniculate leaflet in entrainment of circadian rhythms to a skeleton photoperiod", J Neurosci, 19(1): 372-380.

[25]   Michel, S., Itri, J. and Colwell, C.S. (2002). "Excitatory mechanisms in the suprachiasmatic nucleus: the role of AMPA/KA glutamate receptors", J Neurophysiol, 88(2): 817-828.

[26]   Morin, L.P. (2013). "Neuroanatomy of the extended circadian rhythm system", Exp Neurol, 243: 4-20.

[27]   Dubocovich, M.L. (2007). "Melatonin receptors: role on sleep and circadian rhythm regulation", Sleep Med, 8: S34-S42.

[28]   Claustrat, B., Brun, J. and Chazot, G. (2005). "The basic physiology and pathophysiology of melatonin", Sleep Med Rev, 9(1): 11-24.

[29]   Macchi, M.M. and Bruce, J.N. (2004). "Human pineal physiology and functional significance of melatonin", Front Neuroendocrinol, 25(3-4): 177-195.

[30]   Cardinali, D.P. and Pévet, P. (1998). "Basic aspects of melatonin action", Sleep Med Rev, 2(3): 175-190.

[31]   Von Economo, C. (1930). "Sleep as a problem of localization", J Nerv Ment Dis, 71: 249-259.

[32]   Moruzzi, G. and Magoun, H.W. (1949). "Brain stem reticular formation and activation of the EEG", Electroencephalogr Clin Neurophysiol, 1(4): 455-473.

[33]   Saper, C.B., Scammell, T.E. and Lu, J. (2005). "Hypothalamic regulation of sleep and circadian rhythms", Nature, 437(7063): 1257-1263.

[34]   Lu, J. and Greco, M.A. (2006). "Sleep circuitry and the hypnotic mechanism of GABAA drugs" J Clin Sleep Med, 2(2): S19-26.

[35]   Hobson, J.A., Stickgold, R. and Pace-Schott, E.F. (1998). "The neuropsychology of REM sleep dreaming", Neuroreport, 9(3): R1-14.

[36]   Schwartz, J.R. and Roth, T. (2008). "Neurophysiology of sleep and wakefulness: basic science and clinical implications", Curr Neuropharmacol, 6(4): 367-378.

[37]   España, R.A. and Scammell, T.E. (2011). "Sleep neurobiology from a clinical perspective", Sleep, 34(7): 845-858.

[38]   Fuller, P.M., Saper, C.B. and Lu, J. (2007). "The pontine REM switch: past and present", J Physiol, 584: 735-741.

[39]   Kalia, M. (2006). "Neurobiology of sleep", Metabolism, 55(Suppl 2): S2-6.

[40]   La Salle University, Other types of flip-flops and counting, http://www.lasalle.edu/~blum/p201wks/FlipFlopsAndCounting.ppt, 27 January 2014.

[41]   Armbruster, B.N., Li, X., Pausch, M.H., Herlitze, S. and Roth, B.L. (2007). "Evolving the lock to fit the key to create a family of G protein-coupled receptors potently activated by an inert ligand", Proc Natl Acad Sci USA, 104(12): 5163-5168.

[42]   Pei, Y., Rogan, S.C., Yan, F. and Roth, B.L. (2008). "Engineered GPCRs as tools to modulate signal transduction", Physiology (Bethesda), 23: 313-321.

[43]   Coward, P., Wada, H.G., Falk, M.S., Chan, S.D., Meng, F., Akil, H. and Conklin, B.R. (1998). "Controlling signaling with a specifically designed Gi-coupled receptor", Proc Natl Acad Sci USA, 95(1): 352-357.

[44]   Sweger, E.J., Casper, K.B., Scearce-Levie, K., Conklin, B.R. and McCarthy, K.D. (2007). "Development of hydrocephalus in mice expressing the G(i)-coupled GPCR Ro1 RASSL receptor in astrocytes", J Neurosci, 27(9): 2309-2317.

[45]   Lechner, H.A., Lein, E.S. and Callaway, E.M. (2002). "A genetic method for selective and quickly reversible silencing of Mammalian neurons", J Neurosci, 22(13): 5287-5290.

[46]   Luo, L., Callaway, E.M. and Svoboda, K. (2008). "Genetic dissection of neural circuits", Neuron, 57(5): 634-660.

[47]   Alexander, G.M., Rogan, S.C., Abbas, A.I., Armbruster, B.N., Pei, Y., Allen, J.A., Nonneman, R.J., Hartmann, J., Moy, S.S., Nicolelis, M.A., McNamara, J.O. and Roth, B.L. (2009). "Remote control of neuronal activity in transgenic mice expressing evolved G protein-coupled receptors", Neuron, 63(1): 27-39.

[48]   Peng, J., Bencsik, M., Louie, A., Lu, W., Millard, S., Nguyen, P., Burghardt, A., Majumdar, S., Wronski, T.J., Halloran, B., Conklin, B.R. and Nissenson, R.A. (2008). "Conditional expression of a Gi-coupled receptor in osteoblasts results in trabecular osteopenia", Endocrinology, 149(3): 1329-1337.

[49]   Redfern, C.H., Degtyarev, M.Y., Kwa, A.T., Salomonis, N., Cotte, N., Nanevicz, T., Fidelman, N., Desai, K., Vranizan, K., Lee, E.K., Coward, P., Shah, N., Warrington, J.A., Fishman, G.I., Bernstein, D., Baker, A.J. and Conklin, B.R. (2000). "Conditional expression of a Gi-coupled receptor causes ventricular conduction delay and a lethal cardiomyopathy", Proc Natl Acad Sci USA, 97(9): 4826-4831.

[50]   Hoffman, G.E., Smith, M.S. and Verbalis, J.G. (1993). "c-Fos and related immediate early gene products as markers of activity in neuroendocrine systems", Front Neuroendocrinol, 14(3): 173-213.

[51]   Herrera, D.G. and Robertson, H.A. (1996). "Activation of c-fos in the brain", Prog Neurobiol, 50(2-3): 83-107.

[52]   Garner, A.R., Rowland, D.C., Hwang, S.Y., Baumgaertel, K., Roth, B.L., Kentros, C. and Mayford, M. (2012). "Generation of a synthetic memory trace", Science, 335(6075): 1513-1516.

[53]   Reijmers, L. and Mayford, M. (2009). "Genetic control of active neural circuits", Front Mol Neurosci, 2(27): 1-8.

[54]   McClure, C., Cole, K.L., Wulff, P., Klugmann, M. and Murray, A. J. (2011). "Production and titering of recombinant adeno-associated viral vectors", J Vis Exp, 57: e3348.

[55]   Mastakov, M.Y., Baer, K., Xu, R., Fitzsimons, H. and During, M.J. (2001). "Combined injection of rAAV with mannitol enhances gene expression in the rat brain", Mol Ther, 3(2): 225-232.

[56]   Franklin, K.B.J. and Paxinos, G. (2008). The mouse brain in stereotaxic coordinates, Compact 3rd ed., Editors: Franklin, K.B.J. and Paxinos, G., Elsevier Academic Press, London.

[57]   Vyssotski, A.L., Serkov, A.N., Itskov, P.M., Dell'Omo, G., Latanov, A.V., Wolfer, D.P. and Lipp, H. P. (2006). "Miniature neurologgers for flying pigeons: multichannel EEG and action and field potentials in combination with GPS recording", J Neurophysiol, 95(2): 1263-1273.

[58]   Costa-Miserachs, D., Portell-Cortés, I., Torras-Garcia, M. and Morgado-Bernal, I. (2003). "Automated sleep staging in rat with a standard spreadsheet", J Neurosci Methods, 130(1): 93-101.

[59]   Pang, D.S., Robledo, C.J., Carr, D.R., Gent, T.C., Vyssotski, A.L., Caley, A., Zecharia, A.Y., Wisden, W., Brickley, S.G. and Franks, N.P. (2009). "An unexpected role for TASK-3 potassium channels in network oscillations with implications for sleep mechanisms and anesthetic action", Proc Natl Acad Sci USA, 106(41): 17546-17551.

[60]   Basheer, R., Sherin, J.E., Saper, C.B., Morgan, J.I., McCarley, R.W. and Shiromani, P.J. (1997). "Effects of sleep on wake-induced c-fos expression", J Neurosci, 17(24): 9746-9750.

[61]   Lu, J., Nelson, L.E., Franks, N., Maze, M., Chamberlin, N.L. and Saper, C.B. (2008). "Role of endogenous sleep-wake and analgesic systems in anesthesia", J Comp Neurol, 508(4): 648-662.

[62]   Gent, T.C. (2011). Thalamocortical oscillations in sleep and anaesthesia, PhD. Thesis, Imperial College London (University of London), London.

[63]   Lazarus, M., Chen, J.F., Urade, Y. and Huang, Z.L. (2013). "Role of the basal ganglia in the control of sleep and wakefulness", Curr Opin Neurobiol, 23(5): 780-785.

[64]   Modirrousta, M., Mainville, L. and Jones, B.E. (2004). "Gabaergic neurons with alpha2-adrenergic receptors in basal forebrain and preoptic area express c-Fos during sleep", Neuroscience, 129(3): 803-810.

[65]   Sasaki, K., Suzuki, M., Mieda, M., Tsujino, N., Roth, B. and Sakurai, T. (2011). "Pharmacogenetic modulation of orexin neurons alters sleep/wakefulness states in mice", PLoS One, 6(5): e20360.

[66]   Lazarus, M., Shen, H.Y., Cherasse, Y., Qu, W.M., Huang, Z.L., Bass, C.E., Winsky-Sommerer, R., Semba, K., Fredholm, B.B., Boison, D., Hayaishi, O., Urade, Y. and Chen, J.F. (2011). "Arousal effect of caffeine depends on adenosine A2A receptors in the shell of the nucleus accumbens", J Neurosci, 31(27): 10067-10075.

[67]   Kaur, S., Panchal, M., Faisal, M., Madan, V., Nangia, P. and Mallick, B.N. (2004). "Long term blocking of GABA-A receptor in locus coeruleus by bilateral microinfusion of picrotoxin reduced rapid eye movement sleep and increased brain Na-K ATPase activity in freely moving normally behaving rats", Behav Brain Res, 151(1-2): 185-190.

[68]   Hsieh, K.C., Gvilia, I., Kumar, S., Uschakov, A., McGinty, D., Alam, M.N. and Szymusiak, R. (2011). "c-Fos expression in neurons projecting from the preoptic and lateral hypothalamic areas to the ventrolateral periaqueductal gray in relation to sleep states", Neuroscience, 188: 55-67.

[69] Saper, C.B., Chou, T.C. and Scammell, T.E. (2001). "The sleep switch: hypothalamic control of sleep and wakefulness", Trends Neurosci, 24(12): 726-731.

[70] Saito, Y.C., Tsujino, N., Hasegawa, E., Akashi, K., Abe, M., Mieda, M., Sakimura, K. and Sakurai, T. (2013). "GABAergic neurons in the preoptic area send direct inhibitory projections to orexin neurons.", Front Neural Circuits, 7: 192.

[71] Morairty, S., Rainnie, D., McCarley, R. and Greene, R. (2004). "Disinhibition of ventrolateral preoptic area sleep-active neurons by adenosine: a new mechanism for sleep promotion", Neuroscience, 123(2): 451-457.

CURRICULUM VITAE

PERSONAL INFORMATION

Name Surname	: İlke GÜNTAN
Date of birth and place	: 20/09/1989 KONAK
Foreign Languages	: English, Japanese, Korean
E-mail	: ilkeguntan@gmail.com

EDUCATION

Degree	Department	University	Date of Graduation
Undergraduate	Bioengineering	Yıldız Technical University	August 2011
High School	Science and Mathematics	Izmir Kiz High School	June 2007

WORK EXPERIENCE

Year	Corporation/Institute	Enrollment
2011	Occlutech Medical Devices Industry and Trade Limited Company	Traniee
2009	Istanbul Technical University	Trainee
	Molecular Biology-Biotechnology & Genetics Research Center	

PUBLICATIONS

Conference Papers

1.   Guntan I, Turgut-Balik D. "Effects of genes in daily life and schizophrenia." International-attended ITU 5th National Molecular Biology and Genetics Student Congress, Istanbul Technical University, August 19-22, 2011.

Projects

1.   Guntan I, Allahverdiyev A. "Cellular Apoptosis in Defence of Infectious Diseases", BSc. Project, Yildiz Technical University, Department of Bioengineering, Istanbul.

AWARDS

1.   Erasmus Grant 2012-2013.